SAND76-0427
NUREG766510
Unlimited Release

DISTRIBUTION
CATEGORY NRC-12

Shock and Vibration Environments for Large Shipping Containers on Rail Cars and Trucks

Clifford F. Magnuson, Leonidas T. Wilson

Prepared by Sandia Laboratories, Albuquerque, New Mexico 87115
and Livermore, California 94550, for the United States Nuclear
Regulatory Commission under ERDA Contract E(29-1)-789

Printed July 1977

Sandia Laboratories

Nuclear Fuel Cycle Programs

SF 2900 Q(7-73)

Issued by Sandia Laboratories, operated for the United States Energy Research and Development Administration by Sandia Corporation.

Available from

National Technical Information Service
Springfield, Virginia 22161

DISCLAIMER

SAND76-0427
NUREG766510
Unlimited Release

SHOCK AND VIBRATION ENVIRONMENTS FOR LARGE SHIPPING CONTAINERS ON RAIL CARS AND TRUCKS*

C. F. Magnuson
Applied Mechanics Division II - 1282
L. T. Wilson
Applied Mechanics Division III - 1284

Sandia Laboratories
Albuquerque, New Mexico 87115

Printed June, 1977

ABSTRACT

The purpose of this study was to provide definitions of shock and vibration environment to which fissile material shipping containers may be exposed during normal shipment by truck and rail cars. The definitions of vibration, shock superimposed on vibration and rail coupling shock result from existing data. The dependence of shock environment, from rail coupling operations, on parameters like cargo weight and shock attenuation couplers was also studied using spring-mass models. These studies show that for rail cars equipped with standard draft gear, the cargo response decreases with increased cargo weight until the springs bottom out. For rail cars equipped with shock attenuation couplers, cargo weight has little effect on cargo response. The study also shows the importance of matching couplers and tiedown stiffnesses to decrease the cargo response. Vibration and shock data samples have been obtained during truck shipment of heavy cargo and the data will be presented in subsequent reports. Similar data need to be obtained for rail shipment of heavy cargo and during rail coupling operations with heavy cargo.

*This work was sponsored by the Division of Safeguards, Fuel Cycle and Environmental Research of the United States Nuclear Regulatory Commission; Contract No. A-1049-6.

ACKNOWLEDGEMENTS

The authors gratefully acknowledge the contributions made to this study by C. A. Davidson, J. T. Foley, E. L. Harley, M. Huerta, S. E. Benzley, R. T. Othmer, T. L. Paez, T. G. Priddy, R. Rodeman, and W. A. Von Riesemann.

TABLE OF CONTENTS

TABLES

ILLUSTRATIONS

FOREWORD

Packaging and transport of fissile radioactive materials are regulated by the U.S. Nuclear Regulatory Commission by means of Code of Federal Regulations Title 10, Part 71. Appendix A of these regulations specifies environmental conditions of transport to be applied to determine their effects on packages of radioactive materials. However, the appendix does not specify numerically the frequencies or amplitudes of vibration and shock environments nor does it mention their expected occurrence rate as a function of shipment time and/or mileage. As a result, when evaluating a package for licensing applications, assumptions regarding these environments must be made by each applicant.

To provide guidance in this area, the U.S. Nuclear Regulatory Commission contracted with Sandia Laboratories to gather and evaluate data regarding truck and rail shock and vibration environments normally encountered in transporting large shipping casks. The project is divided into three tasks:

(1) Extract, review, and reduce shock and vibration environment definitions currently on file in both the ERDA/DOD and ERDA Transportation Environment Data Banks. Determine the best, simply stated estimates of environments for large shipping containers on truck and rail car.

(2) Conduct dynamic analyses of the shock environment experienced by cargo in rail switching and coupling to identify the dependence of the shock environment on heavy cargo weights and on shock attenuation couplers. The results are to be used to refine further the shock load description. Existing mathematical models of freight cars will be altered to study these special concerns.

(3) Identify during the performance of Tasks 1 and 2 the need for additional data. The tests which are necessary to obtain these data are to be planned. Actual measurements will be obtained on a "piggyback" basis.

Tasks (1) and (2) are addressed in this report. Task (3) will be addressed in subsequent reports.

All data used in this report as well as the analyses conducted were based on English units. The metric (SI) units presented are approximate conversions from the English units.

SUMMARY

This report contains descriptions of shock and vibration to which shipping containers may be exposed during normal shipment by rail and truck. The data and analyses presented encompass (1) investigations of existing shock and vibration data in the ERDA/DOD and ERDA Transportation Data Banks and (2) analytical studies of the shock environment experienced by cargo to determine the dependence of the environment on cargo weight, tiedowns, and shock attenuation couplers.

Vibration data investigated for this report show the highest expectancy level of cargo vibration to be:

Carrier	Axis	0 to Peak Maximum Acceleration (g)	Frequency Range (Hz)
Truck	Longitudinal	1.50	0 - 1900
	Transverse	1.17	0 - 1900
	Vertical	2.00	0 - 1900
Rail Car	Longitudinal	0.19	0 - 350
	Transverse	0.19	0 - 350
	Vertical	0.37	0 - 350

The shock data investigated show the following simple half-sine input pulses which conservatively represent the maximum expected shock severities:

Carrier	Axis	Peak Acceleration (g)	Pulse Duration (ms)
Truck (Shocks Superimposed on Vibration)	Longitudinal	2.8	20
	Transverse	2.3	19
	Vertical	7.0	77
Rail Car (Shocks superimposed on vibration)	All	4.7	14
Rail Coupling 17.78km/hr (11.05 mph)	Longitudinal	39.0	18
	Vertical	26.0	9

Analyses of coupling operations for two rail shipment combinations, the first a rail car with a representative spent fuel cask system and the second an ATMX car with two radioactive waste material containers, showed that, for rail cars equipped with standard draft

gear, shock environments at the cargo decrease as cargo weight increases until the coupler springs bottom out. For rail cars equipped with shock attenuation couplers, there is little variation in shock severity throughout the range of weights for which the analyses were conducted. These analyses also showed that cargo should be tied securely to the rail car to prevent relative motion between the cargo and the car followed by stiff impact of the cargo against car structure.

CHAPTER I

VIBRATION AND SHOCK ENVIRONMENTS ENCOUNTERED DURING TRUCK AND RAIL TRANSPORTATION

The environmental descriptions presented in this chapter are summaries of data from the ERDA/DOD and ERDA Transportation Data Banks. The data were gathered on different modes of transport for use in defining the environments to which weapons may be exposed. Since about 1960 these data have been obtained from literature sources and, to a large extent, measured, reduced, and analyzed by the Engineering Analysis Department of Sandia Laboratories.

Definitions of Dynamic Environments

Dynamic excitations delivered to cargo may be described as a mixture of vibration, occasional shock superimposed on the vibration and isolated shock which occurs in single events such as rail coupling.

Vibration is the excitation which occurs whenever the carrier is in motion and is produced by the carrier suspension system and carrier frame members reacting to travel over surface irregularities in highways or railroads as well as the vibration generated by the carrier motive system.

Superimposed shock is that which often results in higher amplitudes of cargo response than that produced by vibration. Characteristically it consists of decaying transient pulses which are superimposed and intermixed with the vibration. For trucks the superimposed shock is produced by crossing railroad tracks, bridge approaches, and cattle guards and by striking pot holes. For rail cars the superimposed shock is produced by run-in and run-out and by crossing bridges, switches, and other track intersections.

Shock resulting from rail coupling operations is significantly more severe than that which is superimposed and intermixed with the vibration; however, it occurs less frequently.

Explanation of Data

Vibration definitions presented herein are 0 to peak acceleration amplitude levels which envelope 99 percent of all amplitudes measured in each frequency band. The remaining one percent of the data was

considered to represent superimposed shock and was treated separately. The distribution of the 99 percent acceleration amplitudes in each frequency band is random for which the probability distribution is very nearly Gaussian. The acceleration amplitudes were measured at the interface between the cargo and the cargo floor.

The data for shock were reduced in single-degree-of-freedom response spectra format. These spectra predict the maximum acceleration amplitude at which various single-degree-of-freedom systems would respond when subjected to the transient inputs. Response spectra are used because they permit translation of complex input into a more useful engineering format and permit statistical analysis of diverse individual phenomena. In these response spectra, three percent damping was used because our experience shows this to be representative of the response of metal to metal connections.

Truck Data

Vibration

The vibration data presented were obtained from over-the-road tests using seven different truck and tractor-trailer configurations[1,2]. The trucks were equipped with both conventional spring suspension systems and air-cushioned suspension systems. The cargo weights varied from no load to 133,000 N (15 tons). The trucks traveled over 2-lane highways, interstate highways, and secondary roads. Speeds varied over these different road types.

The highest of the 99 percent 0 to peak acceleration amplitudes of 2 g were found to occur in the vertical axis in the 0 - 5 Hz frequency band. The amplitude levels in the vertical axis decreased to below 1 g between 80 and 700 Hz and then increased to 1.17 g between 700 to 1400 Hz and again decreased to .87 g in the 1400 to 1900 Hz frequency band.

The highest of the 99 percent 0 to peak acceleration amplitude levels of 1.5 g in the longitudinal axis occurred in the 700 to 1000 Hz frequency band. In this axis the second highest amplitude of 1.23 g occurred in the 120 to 180 Hz frequency band. The acceleration amplitudes in all other frequency bands were 0.87 g or lower.

The 99 percent 0 to peak acceleration amplitude levels in the transverse or lateral axis were below 0.42 g up to 700 Hz, increased to 0.87 g in the 700 to 1000 Hz frequency band and 1.17 g in the 1000 to 1400 Hz frequency band, then decreased to 0.24 g in the 1400 to 1900 Hz frequency band. A tabular summary of the 99 percent 0 to peak

acceleration amplitude levels for the three axes discussed above are presented in Table I.

TABLE I

TRUCK VIBRATION

Frequency Band (Hz)	Measurements on Cargo Floor (g) 99% Level of 0 to Peak Amplitude		
	Longitudinal Axis	Transverse Axis	Vertical Axis
0-5	0.10	0.10	2.00
5-10	0.08	0.06	1.04
10-20	0.84	0.15	1.68
20-40	0.51	0.24	1.20
40-80	0.36	0.42	0.50
80-120	0.24	0.27	0.87
120-180	1.23	0.21	0.63
180-240	0.87	0.12	0.87
240-350	0.24	0.15	0.63
350-500	0.24	0.15	0.42
500-700	0.87	0.15	0.87
700-1000	1.50	0.87	1.17
1000-1400	0.87	1.17	1.17
1400-1900	0.39	0.24	0.87

Shock

The shock data presented were obtained from the same tests as the truck vibration data, but from different events. The shock data were obtained from measurements taken when the trucks encountered potholes, railroad crossings, and bridge approaches. The data presented define the response at the interface of the cargo and the cargo floor.

The vertical axis produced the highest predicted cargo response of the three axes across the complete frequency spectrum from 1 to 150 Hz. The predicted cargo response in the other two axes are very similar to each other. The response spectra for all three axes are shown in Figure 1. Surveys of interstate highways in Colorado, Utah, Wyoming, and New Mexico show a potential of superimposed shock-producing road irregularities occurring approximately once per 1.61 km (one mile) of travel.

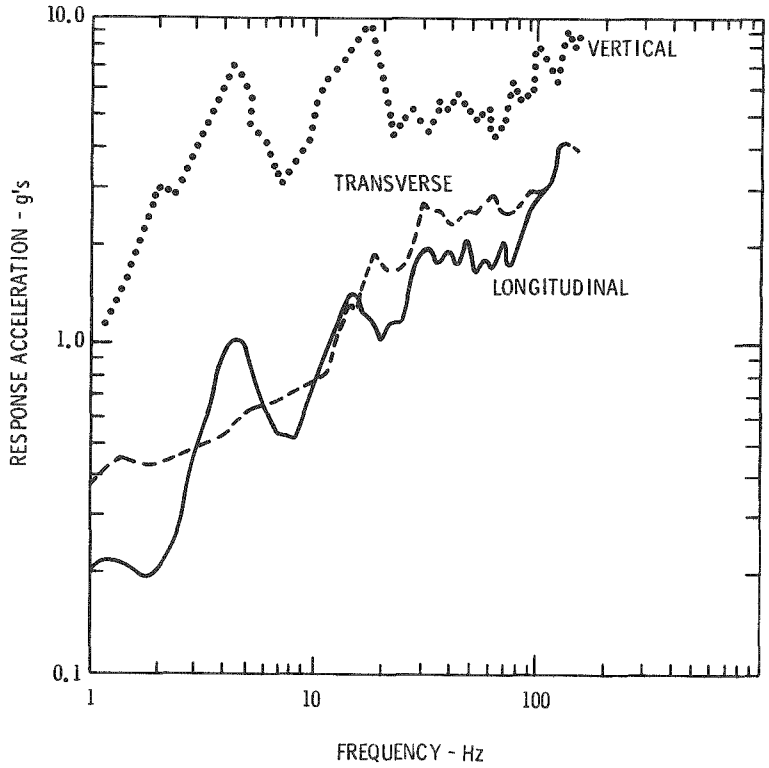

Figure 1. Truck Superimposed Shock Response Envelopes -- 3% Damping

Rail Data

Vibration

The vibration data presented herein were obtained during a shipment of a 133,000 N (15-ton) fuel cask positioned at the center of a USAX car[3]. The shipment was made over normal rail routes from Paducah, Kentucky to Oak Ridge, Tennessee. The cask was tied down by tie-rods which extended through the floor of the car and attached to plates which had been welded to the car frame. The instrumented rail car was attached to three different trains. Their lengths varied from 65 to 120 cars during the trip.

The highest 99 percent 0 to peak acceleration amplitude level of 0.37 g occurred in the vertical axis. The vertical axis produced the same as or greater acceleration amplitudes than the other axes over the entire frequency spectrum of 0 to 350 Hz. The amplitude levels are generally lower than for trucks in all three axes and do not vary significantly over the 0 to 350 Hz frequency spectrum. Data were not reduced above 350 Hz but interpretations indicated that the acceleration amplitude distributions above 350 Hz are similar to those in the 250

to 350 Hz frequency band. Details of the 0 to peak acceleration amplitudes which encompass 99 percent of vibrations in specified frequency bands between 0 and 350 Hz are presented in Table II.

TABLE II

TRAIN VIBRATION

Frequency Band (Hz)	Measurements on Cargo Floor (g) 99% Level of 0 to Peak Amplitude		
	Longitudinal Axis	Transverse Axis	Vertical Axis
0-5	0.14	0.14	0.37
5-10	0.072	0.072	0.14
10-20	0.072	0.072	0.10
20-30	0.10	0.10	0.27
30-45	0.19	0.14	0.37
45-60	0.10	0.10	0.27
60-87	0.10	0.19	0.19
87-125	0.10	0.19	0.19
125-175	0.10	0.10	0.19
175-250	0.10	0.14	0.14
250-350	0.10	0.10	0.14

In a report describing research rail vibration tests conducted on specially prepared tracks[4], it was concluded that as cargo weight on rail cars increases, vibration amplitudes in the car body decrease. To determine the trend of this reduction over normal railroad routes, additional tests with heavy cargo need to be conducted.

Shock

The shock descriptions presented are shown in single-degree-of-freedom response spectra as was done for trucks. Two shock descriptions for rail are provided. The first is for shock which is superimposed on vibration and the second is for shock resulting from rail coupling operations.

Superimposed Shock - The data presented for shock which is superimposed on vibration were obtained during the same test described under rail vibration, but for different events. These events included crossing rail joints, traveling through switches, and run-in and run-out. The data describe the response at the interface of the cargo and the cargo floor.

The levels of response are similar in all three axes in the frequency range between 3 and 150 Hz for which data were reduced. The response spectra envelopes for all three axes are shown in Figure 2. Analysis of data obtained during train transport of cars which were uniformly loaded with heavy cargo shows run-in and run-out events which may produce the levels of response shown occurring at an average rate of 9 times per 161 km (100 miles) of travel. Data to provide estimates for the frequency of crossing rail joints and travel through switches are not available.

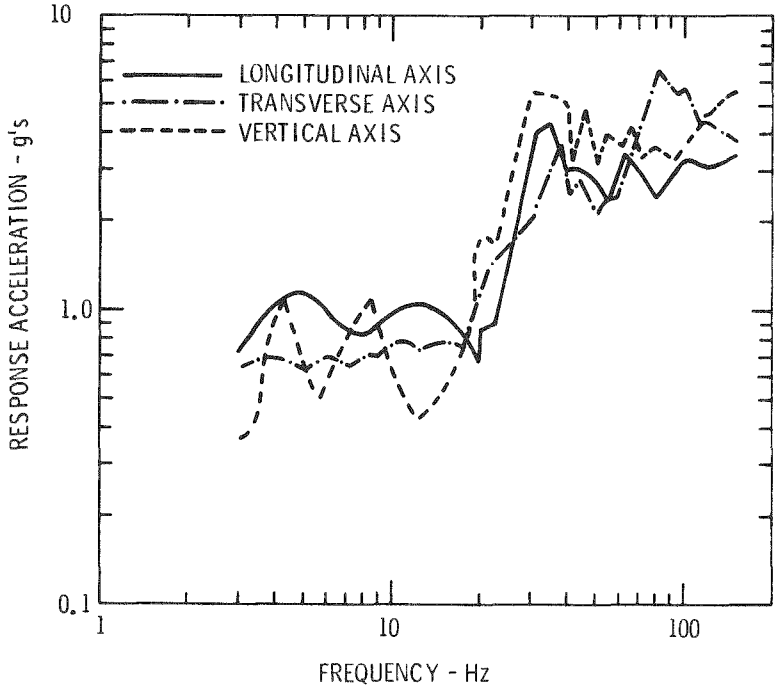

Figure 2. Rail Superimposed Shock Response Envelopes -- 3% Damping

Rail Coupling Shock - Data for rail coupling shock were obtained from tests which had been conducted in the early 1960's using ATMX cars. The cargo was relatively light (approximately 44,500 N (10,000 pounds) to represent weapons. These tests were conducted at coupling speeds of 8.45, 10.78, 14.21, and 17.78 km/hr (5.25, 6.7, 8.83, and 11.05 mph respectively). Compilation of data from 15,648 switching and coupling operations[5,6,7,8] presented in Table III showed that 63.5 percent of the observed coupling velocities were below 8.45 km/hr (5.25 mph); nearly 90 percent were at or below 10.78 km/hr (6.7 mph); 98 percent

were below 14.21 km/hr (8.83 mph); and 99.8 percent were below 17.78 km/hr (11.05 mph).

Data obtained from the tests were considered applicable for presentation in this report even though the Code of Federal Regulations (CFR) 49, Part 174.589(c) states that cars transporting radioactive material are to be coupled together with a force no greater than that necessary to complete the coupling. This force is not specified.

Rail cars are designed to withstand impacts which produce 5,560,300 N (1,250,000 pounds force) at the coupler or impact velocities up to 22.53 km/hr (14 mph)[9] and the observed coupling operations included impact velocities of 27.36 km/hr (17 mph) with 99.8 percent at or below 17.70 km/hr (11 mph).

TABLE III

OBSERVED IMPACT VELOCITIES DURING RAIL COUPLING

Observed Impact Speeds (km/hr)	(mph)	Number Reported	Percent of Total	Cumulative Percent
≤ 8.05	≤ 5	9936	63.5	63.5
9.66	6	2831	18.1	81.6
11.27	7	1331	8.5	90.1
12.87	8	748	4.8	94.9
14.48	9	492	3.1	98.0
16.09	10	208	1.3	99.3
17.70	11	73	0.5	99.8
19.31	12	1	0.01	99.8
20.92	13	20	0.1	99.9
22.53	14	3	0.02	99.9
24.14	15	3	0.02	99.9
25.75	16	0	0	99.9
27.36	17	2	0.01	100.0

The response spectra for the ATMX car tests are shown in Figures 3 through 10. They cover the vertical and longitudinal axes for the four impact velocities of the tests. These data combine to define the response at the interface between the cargo and the cargo floor. The data for the transverse axis were so low that they were not reduced.

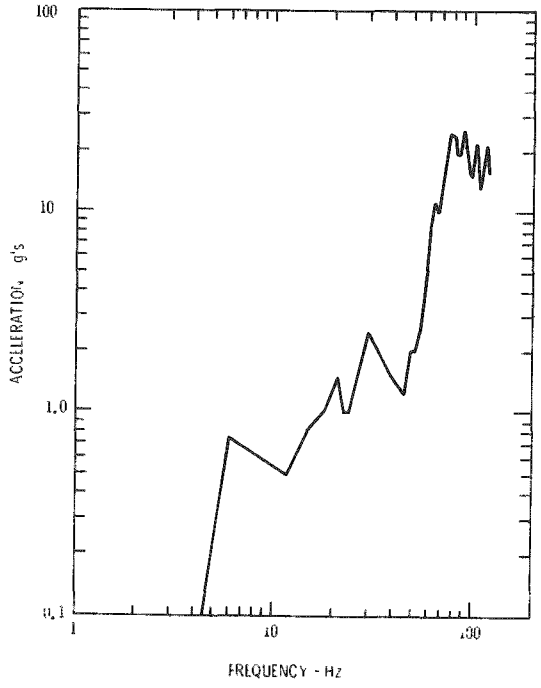

Figure 3. Railroad Coupling Shock Response Spectrum--3% Damping -- ATMX-500 -- 8.45 km/hr (5.25 mph) Impact -- Vertical Axis

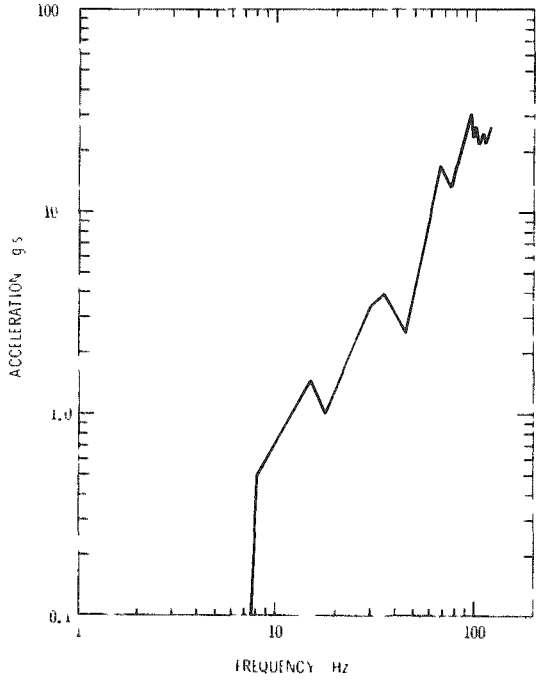

Figure 4. Railroad Coupling Shock Response Spectrum -- 3% Damping -- ATMX-500 -- 10.78 km/hr (6.7 mph) Impact -- Vertical Axis

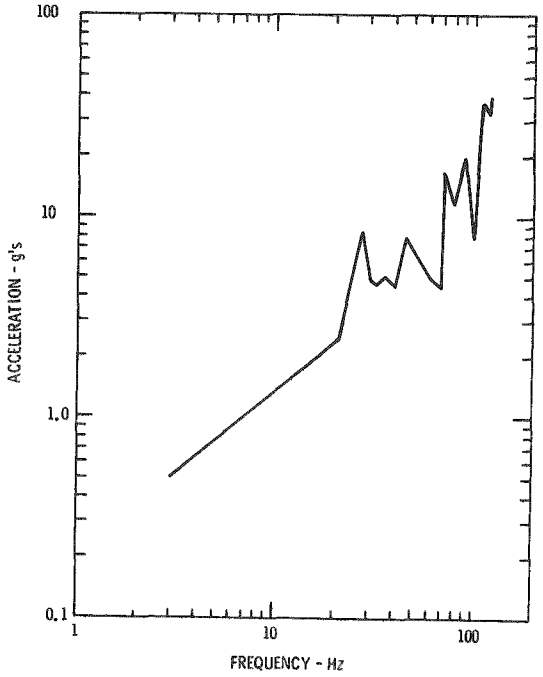

Figure 5. Railroad Coupling Shock Response Spectrum -- 3% Damping -- ATMX-500 -- 14.21 km/hr (8.83 mph) Impact -- Vertical Axis

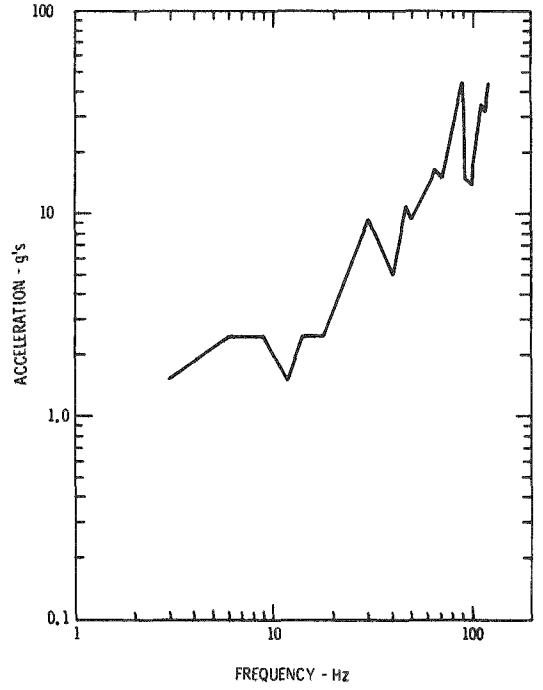

Figure 6. Railroad Coupling Shock Response Spectrum -- 3% Damping -- ATMX-500 -- 17.78 km/hr (11.05 mph) Impact -- Vertical Axis

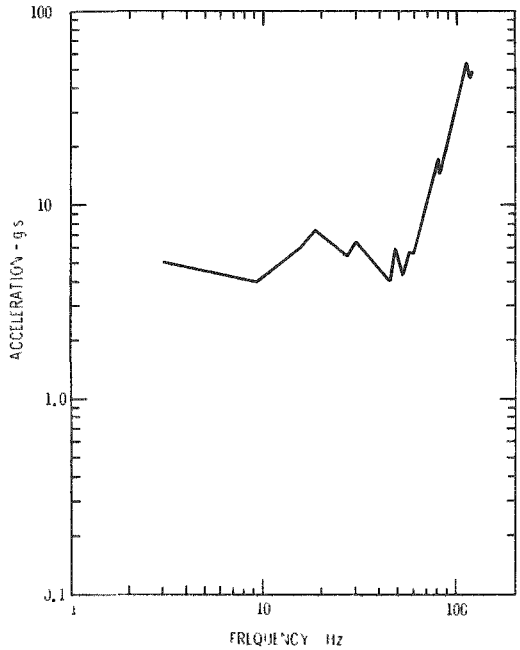

Figure 7. Railroad Coupling Shock Response Spectrum -- 3% Damping -- ATMX-500 -- 8.45 km/hr (5.25 mph) Impact - Longitudinal Axis

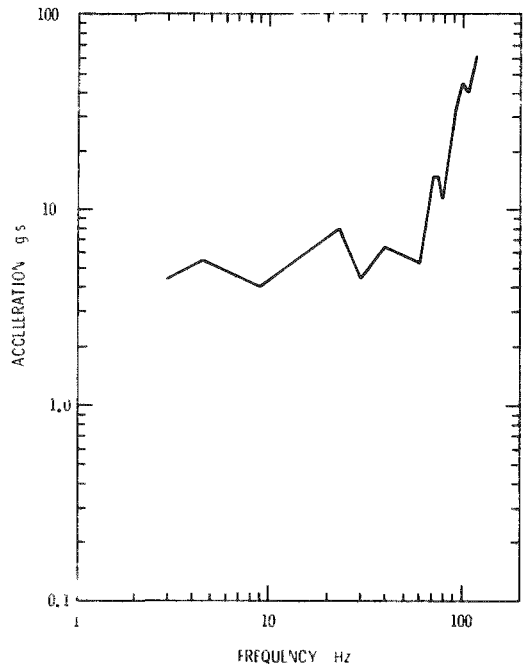

Figure 8. Railroad Coupling Shock Response Spectrum -- 3% Damping -- ATMX-500 - 10.78 km/hr (6.7 mph) Impact -- Longitudinal Axis

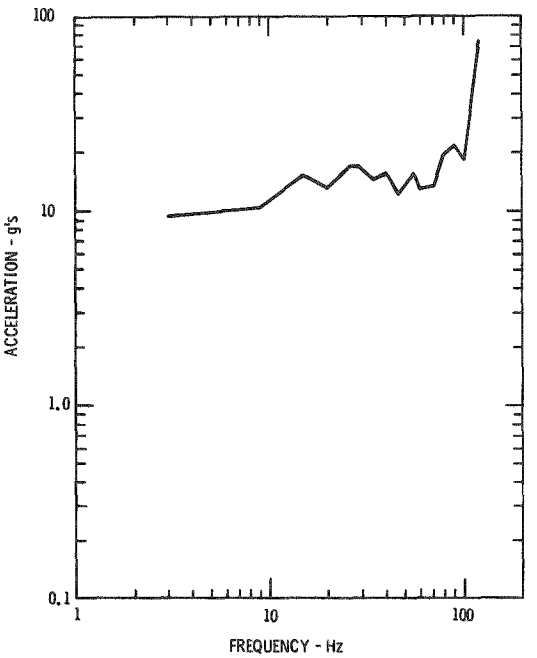

Figure 9. Railroad Coupling Shock Response Spectrum -- 3% Damping -- ATMX-500 -- 14.21 km/hr (8.83 mph) Impact -- Longitudinal Axis

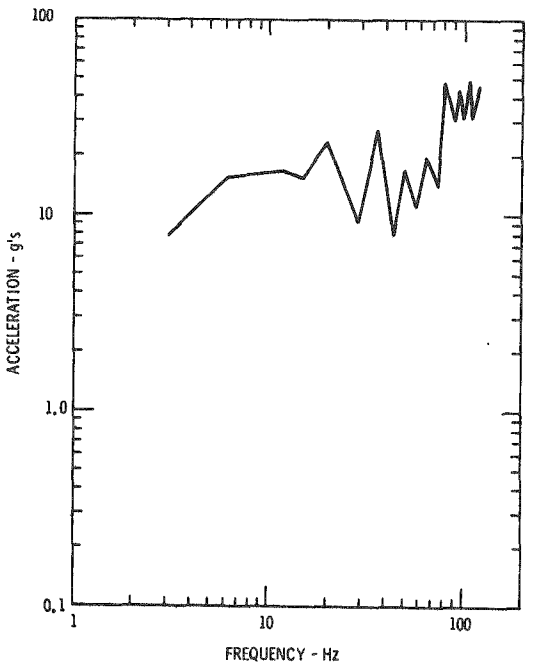

Figure 10. Railroad Coupling Shock Response Spectrum -- 3% Damping -- ATMX-500 -- 17.78 km/hr (11.05 mph) Impact -- Longitudinal Axis

CHAPTER II
SINGLE PULSE REPRESENTATION OF SHOCK

To simplify shock definition for evaluation of mechanical systems, it is convenient to approximate the complex inputs caused by shock with single simple pulses. In this chapter the method for deriving these simple pulses is discussed and specific pulses which produce response spectra that envelope those obtained from the tests reported in Chapter I are presented. These input pulses represent the input shock encountered in normal truck and rail transport.

Method

Simple pulses to represent input shock are derived by comparing response spectra generated from test data or analyses with the response spectrum from a single pulse. This comparison usually introduces conservatism because the response spectra from test data are enveloped by the single pulse response spectrum up to the highest frequency of interest. Several simple pulse shapes can be selected to define an input pulse. In this report, half-sine pulses are used.

An overlaying technique is used to derive the peak acceleration and pulse duration of a single half-sine input pulse to represent the complex shock pulse. In this technique, the response spectrum from the half-sine pulse is normalized by plotting the ratios of response acceleration to input acceleration against the ratio of response frequency to input frequency (Figure 11). The normalized response spectrum, computed with the same damping as the test spectrum, is then overlaid on the test spectrum so as to envelope the acceleration values of interest. The peak acceleration for the derived single pulse is taken from the point on the resulting plot where the value of the ratio of accelerations from the normalized response spectrum is one. The pulse duration is obtained in a similar manner from the inverse of the frequency at the point where the value of the ratio of frequencies is one (Figure 12). The component of velocity change which results from the exchange of energy from the simple pulse can be calculated. The velocity change, which is represented by the area under the curve of the half-sine pulse, is used to evaluate the reasonableness of the specific pulse selected for each application.

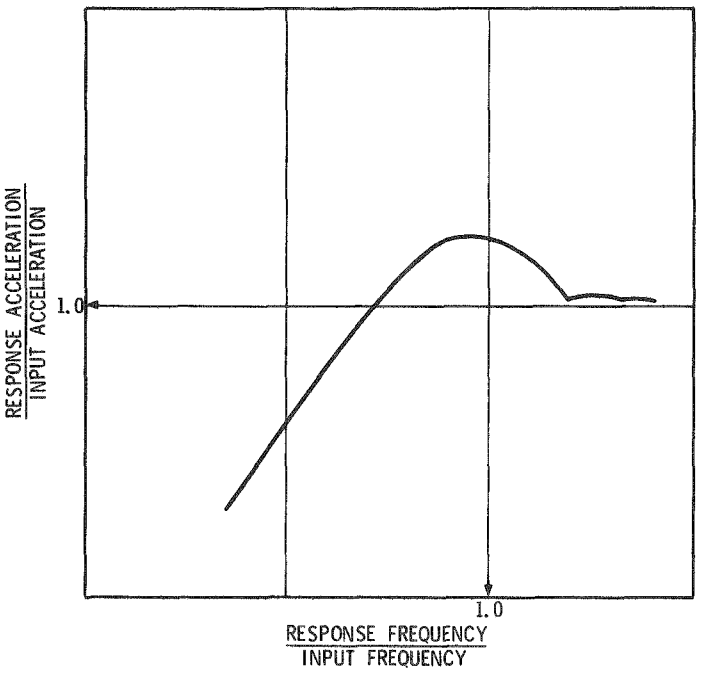

Figure 11. Normalized Single Degree of Freedom Response Spectrum Half-Sine Pulse - 3% Damping

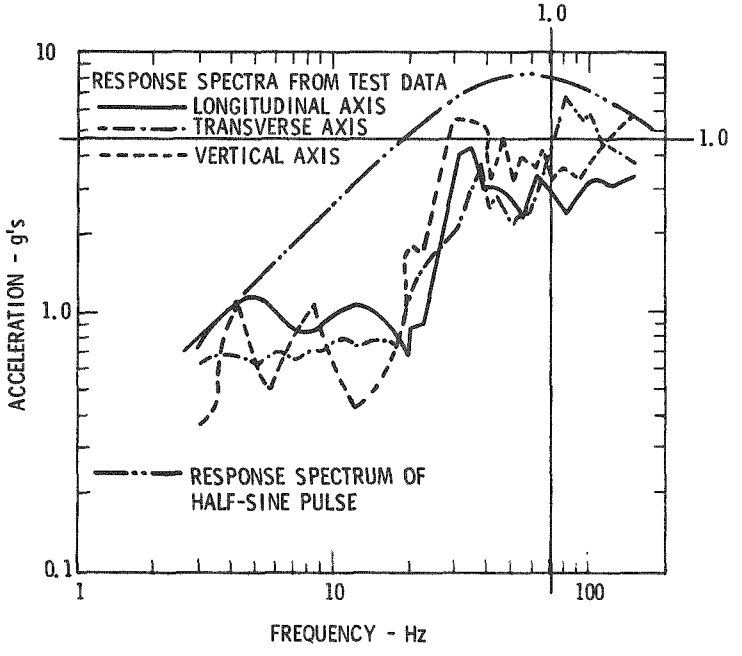

Figure 12. Test Data Response Spectra Enveloped by Simple Pulse Response Spectrum

Shock Represented by Single Half-Sine Pulses

Truck

Definitions of half-sine pulses which produce response spectra that envelope test response spectra for truck transport were developed using the technique described. The overlay fit was established for each of the three axes. The highest peak acceleration of the input pulses (7g) is in the vertical axis. The peak acceleration of input pulses in the longitudinal and transverse axes are similar in amplitude (2.8 and 2.3 g respectively). The pulse durations are those which provided the best fit for environmental data. The definitions are provided in Table IV.

TABLE IV

TRUCK/SHOCK-REPRESENTED BY SINGLE HALF-SINE PULSES

Axis	Peak Acceleration (g)	Pulse Duration (ms)	Velocity Change (m/sec)	Velocity Change (ft/sec)
Longitudinal	2.8	20	.34	1.1
Transverse	2.3	19	.27	0.9
Vertical	7.0	77	3.32	10.9

Rail

Rail Shock Superimposed on Vibration - The response spectra obtained for rail shock which is superimposed on vibration are similar to each other in acceleration vs frequency content. Therefore, one simple input half-sine pulse having a response spectrum that envelopes the test response spectra was considered adequate for describing the shock in all three axes (Table V).

Rail Shock from Coupling Operations - Single half-sine pulses having response spectra which envelop the test response spectra resulting from rail coupling tests were defined. The peak accelerations and pulse durations are those which resulted from fit of a normalized response spectrum from a half-sine pulse over the spectra from test data. Test data were not reduced in the transverse axis because the response in that axis was much less than in the longitudinal and transverse axes.

The peak accelerations of the single input half-sine pulses for the vertical axis increased from 15 g at 8.45 km/hr (5.25 mph) coupling velocity to 26 g at 17.78 km/hr (11.05 mph) coupling velocity. The peak accelerations of single input half-sine pulses for the longitudinal axis increased from 33 g at 8.45 km/hr (5.25 mph) coupling velocity to 51 g at 14.21 km/hr (8.83 mph) coupling velocity, but then decreased to 39 g at 17.78 km/hr (11.05 mph) coupling velocity. The specific definitions of single input pulses for rail coupling shock are shown in Table V.

TABLE V

RAIL SHOCK-REPRESENTED BY SINGLE HALF-SINE PULSES

Shock Source	Coupling Velocity (km/hr)	Coupling Velocity (mph)	Axis	Peak Acceleration (g)	Pulse Duration (ms)	Velocity Change (m/sec)	Velocity Change (ft/sec)
Superimposed on vibration	NA		All	4.7	14	.40	1.3
Coupling Operations	8.45	5.25	Longitudinal	33	11	2.26	7.4
			Vertical	15	8	.73	2.4
	10.78	6.70	Longitudinal	38	10	2.35	7.7
			Vertical	18	7	.79	2.6
	14.21	8.83	Longitudinal	51	12	3.78	12.4
			Vertical	20	10	1.25	4.1
	17.78	11.05	Longitudinal	39	18	4.33	14.2
			Vertical	26	9	1.43	4.7

CHAPTER III

DYNAMIC ANALYSIS OF SHOCK ENVIRONMENT OF RAIL CARS DURING COUPLING OPERATIONS

Rail coupling operations produce shock environments significantly more severe than those resulting from other truck and rail operations. Therefore, the shock environment experienced by cargo during coupling of rail cars was analyzed to identify the dependence of the environment on parameters such as cargo weight and shock attenuation couplers. Descriptions of the shock environments are presented in terms of half-sine input pulses as was done in the previous chapter for lightweight cargos. The descriptions were obtained by calculating response spectra from mathematical models derived from the structural characteristics of the systems analyzed. The analysis shows that for rail cars equipped with standard draft gear, shock environments at the cargo decrease as cargo weight increases until the coupler springs bottom out. For rail cars equipped with shock attenuation couplers, there is little variation in shock severity throughout the range of weights for which the analysis was conducted. Further, the data show that the cargo should be tied securely to the car to prevent any relative motion between the cargo and the car followed by stiff impact of the cargo against car structure.

Descriptions of the systems analyzed, mathematical models used, and the results of the analysis follow.

Spring-Mass Mathematical Models

Spring-mass models of two rail cars, a representative spent fuel cask system and the ATMX car were developed for the analyses. These models were used in a computer program to produce mathematically the shock descriptions in terms of acceleration vs time at the interface between the cargo and the carrier floor. Shock response spectra were developed from the shock description at this interface.

Spent Fuel Cask System

The spent fuel cask system was assumed to consist of a fuel cask on a skid and a rail car having a cast steel underframe. The rail car was equipped with Freightmaster Type E-15 hydraulic shock attenuation end-of-car couplers. The skid had a receptacle through which a shear structure on the rail car protrudes when the skid rests on the car floor. Clearances of 3.2 mm (1/8 inch) between the shear

structure on the car and the receptacle in the skid were assumed, as shown in Figure 13.

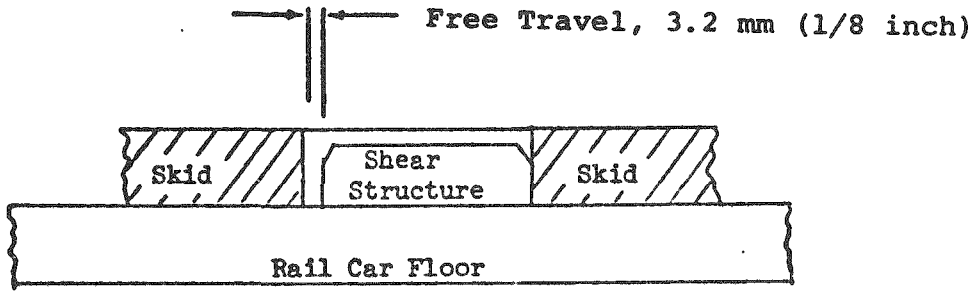

Figure 13. Shear Structure Clearance on Assumed Spent Fuel Cask System

The spent fuel cask system would be used to transport spent fuel by rail and to provide some shock attenuation during coupling. The rail car weighed 289,000 N (65,000 pounds); the container and skid weighed from 178,000 N (40,000 pounds) to 890,000 N (200,000 pounds).

Mathematical Model -- The rail car model was divided into seven masses which were determined by cross bracing and other characteristics of the car structure. The masses were connected in the model by springs with rates calculated from the relationship:

$$K = AE/\ell$$

where A = cross sectional area of structure connecting the masses

E = modulus of elasticity of the material used for connecting structure

ℓ = distance between mass centers

The cask was represented by a single mass located at the shear structure. The space between the shear structure and the skid was included as free travel in the spring rate for the spring between the cargo and the cargo floor. A separate mass of 801,000 N (180,000 pounds) was used to represent a second loaded car into which the model car was coupled. The coupler on the second car was considered to be rigid so

that a worst case situation could be studied. The model, showing associated masses and spring rates, is diagrammed in Figure 14.

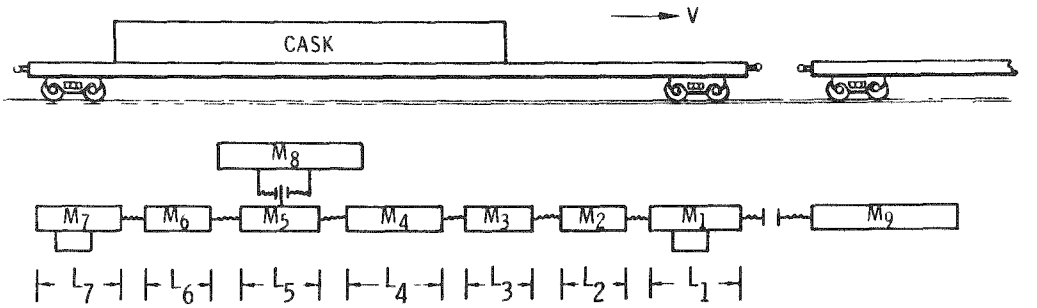

MODEL CHARACTERISTICS

	WEIGHT* (N)	WEIGHT* (lbs)	LENGTH (m)	LENGTH (in)
M_1	78100	(17553)	L_1 = 2.67	(105)
M_2	22600	(5079)	L_2 = 2.44	(96)
M_3	23600	(5301)	L_3 = 1.83	(72)
M_4	41100	(9237)	L_4 = 2.44	(96)
M_5	23600	(5301)	L_5 = 1.83	(72)
M_6	22600	(5079)	L_6 = 2.44	(96)
M_7	78100	(17553)	L_7 = 2.67	(105)
M_8	= (1) 178000	(40000)		
	= (2) 445000	(100000)		
	= (3) 712000	(160000)		
	= (4) 890000	(200000)		
M_9	801000	(180000)		

SPRING RATES

K_{1-2} = 8.98×10^9 N/M(.5130 x 10^8 lb/in)

K_{2-3} = 9.95×10^9 N/M(.5684 x 10^8 lb/in)

K_{3-4} = 16.21×10^9 N/M(.9256 x 10^8 lb/in)

K_{4-5} = 16.21×10^9 N/M(.9256 x 10^8 lb/in)

K_{5-6} = 9.95×10^9 N/M(.5684 x 10^8 lb/in)

K_{6-7} = 8.98×10^9 N/M(.5130 x 10^8 lb/in)

K_{1-9} @ 17.78 km/hr(11.05mph) F = 1712570N(385000lb)

K_{5-8} = 1.75×10^9 N/M(.1000 x 10^8 lb/in)

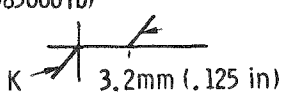

SEE PAGE 4, PAR. 3.4.1.2 OF ASTM METRIC PRACTICE GUIDE E380-72

Figure 14. Spring-Mass Model; Spent Fuel Cask System

ATMX Car

The ATMX rail car was specially designed by Sandia Laboratories for transporting weapons. The car is built on a cast steel underframe of a flat car and is equipped with Miner RF-333 draft gear. The system analyzed included two Dow Chemical Company containers designed to transport radioactive waste material. These containers are fastened to the car floor by heavy brackets[10]. The rail car weighs 525,000 N (118,000 pounds) and the two containers weigh 451,000 N (101,300 pounds) for a total of 975,000 N (219,300 pounds).

Mathematical Model -- The rail car model was divided into seven masses which were determined by the car structure. The masses were connected in the model by springs calculated by the relationship defined for the spent fuel cask system. The spring rate at the coupler was adjusted until the response spectrum from the model was similar to an envelope of response spectra from test data (Figure 15).

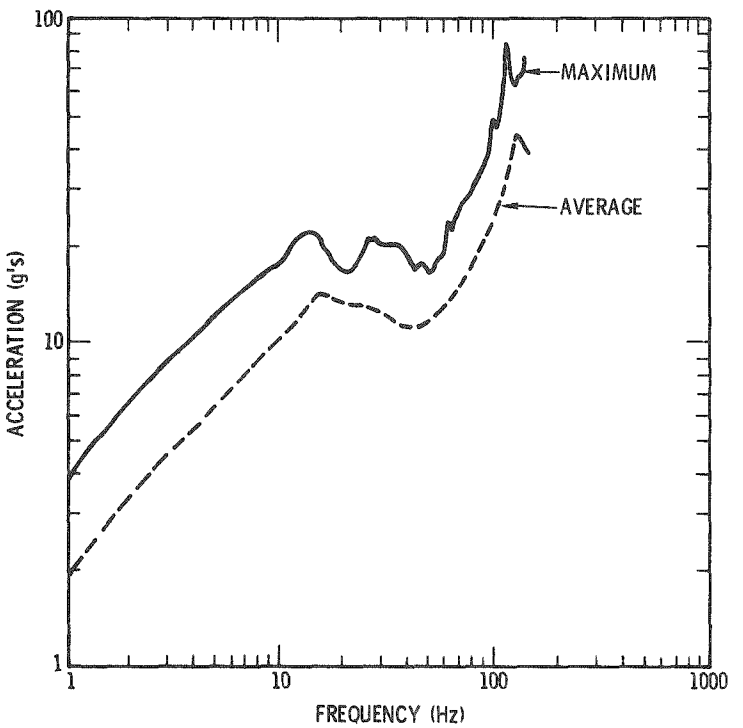

Figure 15. Shock Response Spectra - ATMX-500 and ATMX-600 Composite Spectra - 3% Damping - 17.7 km/hr (11 mph) Impact - Longitudinal Axis

The test data were derived from 10 coupling tests of lightly loaded cars at impact speeds of 17.7 km/hr (11 mph). The spring rate for the cargo tiedowns was estimated from an analysis of the bolts holding anti-skid brackets at the attachment to the cargo floor. Each cask was represented by a mass at the tiedown point on the car. The weights of each cask were varied from 89,000 N (20,000 pounds) to 445,000 N (100,000 pounds). The second car into which the model car was coupled was assigned a mass of 890,000 N (200,000 pounds). Again, the coupler of the second car was assumed to be rigid to present a worst case. The model, associated masses, and spring rates are shown in Figure 16.

Analytical Results

An impact velocity of 17.78 km/hr (11.05 mph), which covers 99.8 percent of observed rail coupling impacts, was used in the analysis. Single-degree-of-freedom response spectra were produced for each of the models with the different cargo weights. These spectra are presented in the Appendix. From these spectra, simple half-sine input pulses calculated with 3 percent damping and having response spectra that envelope the spectra from the analytical models were determined.

Spent Fuel Cask System

The spent fuel cask system responds at approximately 50 to 60 Hz. Response spectra for half-sine input pulses were fitted to the analytical response spectra through 90 Hz. Enveloping from 0 to 90 Hz allows for uncertainty in the natural frequency of the system studied and permits using the half-sine input pulses for systems whose natural frequencies lie within the 0 to 90 Hz range.

During evaluation of the response of the spent fuel cask system, it was noted that in the 50 to 60 Hz frequency region, the response of the rail car structure increased as the weight of the cargo increased. The increased response was caused by the base of the skid moving against the shear structure on the car. At the end of 3.2 mm of free travel between the skid and the shear structure, the skid impacted the shear structure and excited the natural frequencies of the car. Therefore, as the cargo mass became greater, the force available to excite the car structure became greater. As cargo weight increases, higher peak accelerations of the simple pulses are required to envelope the response spectra of the car structure. Results of the analysis are shown in Table VI.

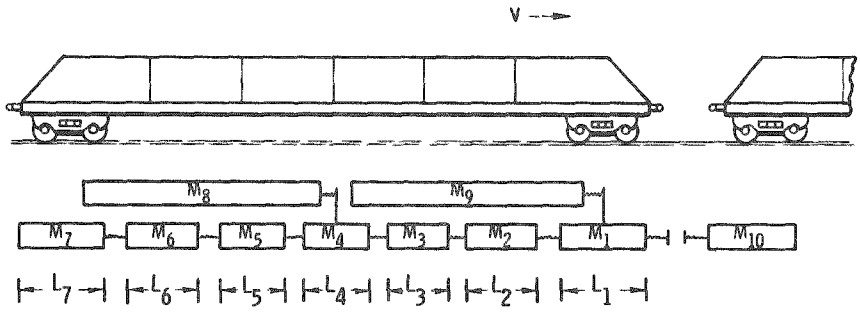

MODEL CHARACTERISTICS

	WEIGHT* (N)	(lbs)		LENGTH (m)	(in)
M_1 =	91200	(20500)	L_1 =	2.90	(114)
M_2 =	68900	(15500)	L_2 =	2.44	(96)
M_3 =	68900	(15500)	L_3 =	2.77	(109)
M_4 =	68900	(15500)	L_4 =	2.13	(84)
M_5 =	68900	(15500)	L_5 =	2.77	(109)
M_6 =	68900	(15500)	L_6 =	2.44	(96)
M_7 =	91200	(20500)	L_7 =	2.90	(114)
$M_8 = M_9$ = (1)	89000	(20000)			
(2)	225300	(50650)			
(3)	356000	(80000)			
(4)	445000	(100000)			
M_{10} =	890000	(200000)			

SPRING RATES

K_{1-2} = 1.75×10^{10} N/M (.1000 x 10^9 lb/in)
K_{2-3} = 2.10×10^{10} N/M (.1200 x 10^9 lb/in)
K_{3-4} = 2.98×10^{10} N/M (.1700 x 10^9 lb/in)
K_{4-5} = 2.98×10^{10} N/M (.1700 x 10^9 lb/in)
K_{5-6} = 2.10×10^{10} N/M (.1200 x 10^9 lb/in)
K_{6-7} = 1.75×10^{10} N/M (.1000 x 10^9 lb/in)
K_{1-10} k_a = 7.00×10^8 N/M (.4000 x 10^7 lb/in)
k_b = 2.10×10^7 N/M (.1200 x 10^6 lb/in)
k_c = 10.51×10^7 N/M (.6000 x 10^6 lb/in)
k_d = 8.76×10^7 N/M (.5000 x 10^6 lb/in)
k_e = 12.26×10^7 N/M (.7000 x 10^6 lb/in)
K_{1-9}, K_{4-8} = 4.95×10^{10} N/M (.2827 x 10^9 lb/in)

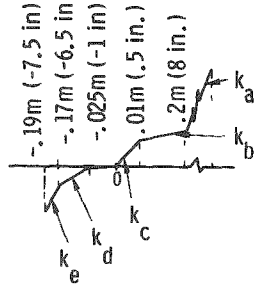

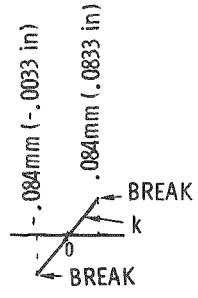

*SEE PAGE 4, PAR. 3.4.1.2 OF ASTM METRIC PRACTICE GUIDE E380-72

Figure 16. Spring-Mass Model;
ATMX-600 Rail Car with Two Fuel Casks

TABLE VI

HALF-SINE PULSES FOR THE SPENT FUEL CASK SYSTEM WITH 3.2 mm FREE TRAVEL SPACE

Cargo Weight (N)	(lbs)	Peak Acceleration (g's)	Pulse Duration (msec)	Velocity Change (m/sec)	(ft/sec)
178,000	40,000	52	13	4.18	13.7
445,000	100,000	58	13	4.66	15.3
712,000	160,000	63	13	5.06	16.6
890,000	200,000	64	13	5.15	16.9

The free travel space between the skid and the shear structure was eliminated in the model to determine the effects on the shock response if the skid were rigidly tied down. This resulted in lowering the response from that of the system with free travel in the 50 to 60 hz region but increasing the response in the 30 to 40 Hz region. The overall result, however, was a decrease in the peak acceleration of half-sine pulses whose response spectra envelop the response spectra developed for the modified spent fuel cask system.

The constant force vs displacement characteristic of the hydraulic end-of-car coupler resulted in peak accelerations of the half-sine input pulses having the same amplitude over the range of weights for which the study was conducted. The pulse durations of the input pulses were changed from those of the preceding model to provide an equally good fit without introducing additional conservatism and to maintain reasonable velocity changes. The results are shown in Table VII.

TABLE VII

HALF-SINE PULSES FOR THE SPENT FUEL CASK SYSTEM WITH CASK TIED DOWN

Cargo Weight (N)	(lbs)	Peak Acceleration (g's)	Pulse Duration (msec)	Velocity Change (m/sec)	(ft/sec)
178,000	40,000	49	14	4.24	13.9
445,000	100,000	49	14	4.24	13.9
712,000	160,000	49	14	4.24	13.9
890,000	200,000	49	14	4.24	13.9

A comparison of the peak acceleration of the half-sine input pulses for the spent fuel cask system with and without the free space between the skid and the shear structure is shown in Figure 17.

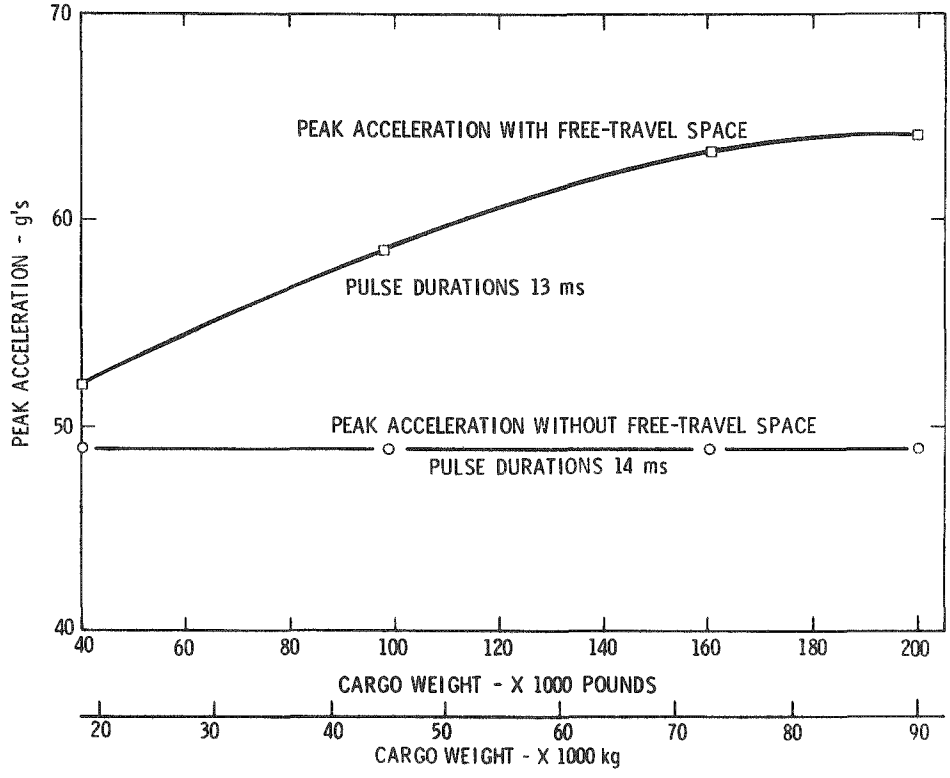

Figure 17. Peak Acceleration and Pulse Duration Half-Sine Pulses - Spent Fuel Cask System Longitudinal Axis

ATMX Car

The ATMX car tiedown structure responds at approximately 100 Hz. Again, response spectra for half-sine input pulses were fitted to analytical response spectra to cover higher frequencies. In this case fitting the half-sine response spectra at 100 Hz resulted in the analytical response spectra being enveloped to 200 Hz. Enveloping to 200 Hz allows for uncertainty in the natural frequency of the ATMX system studied and permits using these half-sine pulses for systems whose natural frequencies lie within the 0 to 200 Hz frequency range. The peak accelerations of the simple input pulses decreased as cargo weight increased up to 712,000 N (160,000 pounds) and then increased at 890,000 N (200,000 pounds) cargo weight. The higher peak accelerations of the input pulses which are required to envelop the response spectra of the lighter cargo analytical response spectra result from

more violent reaction of the smaller masses to the springs in the spring-mass model. The high peak acceleration at 890,000 N (200,000 pound) cargo weight results from bottoming out of the coupler spring which creates greater excitation in the tie-down structure. The results are shown in Table VIII.

TABLE VIII

HALF-SINE PULSES FOR ATMX SYSTEM WITH STANDARD DRAFT GEAR

Cargo Weight (N)	(lbs)	Peak Acceleration (g's)	Pulse Duration (msec)	Velocity Change (m/sec)	(ft/sec)
178,000	40,000	75	10	4.63	15.2
451,000	101,300	55	10	3.41	11.2
712,000	160,000	45	10	2.77	9.1
890,000	200,000	55	10	3.41	11.2

The model of the ATMX car was revised to include the characteristics of the .38 metre (15-inch) hydraulic shock attentuation end-of-car couplers which are a part of the spent fuel cask system. This was done to determine the effects on the cargo if the ATMX car was equipped with these devices. As on the spent fuel cask system, the analytical response spectra were about constant over the range of weights for which the study was conducted (Table IX). However, the magnitude of the peak acceleration was higher for the ATMX car because the end-of-car coupler and tiedown stiffness were not compatible.

TABLE IX

HALF-SINE PULSES FOR ATMX SYSTEM WITH .38 METRE (15-INCH) HYDRAULIC END-OF-CAR COUPLERS

Cargo Weight (N)	(lbs)	Peak Acceleration (g's)	Pulse Duration (msec)	Velocity Change (m/sec)	(ft/sec)
178,000	40,000	80	10	4.94	16.2
451,000	101 300	80	10	4.94	16.2
712,000	160,000	80	10	4.94	16.2
890,000	200,000	80	10	4.94	16.2

A comparison of the half-sine input pulses for the ATMX car equipped with standard draft gear and .38 metre (15-inch) hydraulic end-of-car couplers is shown in Figure 18.

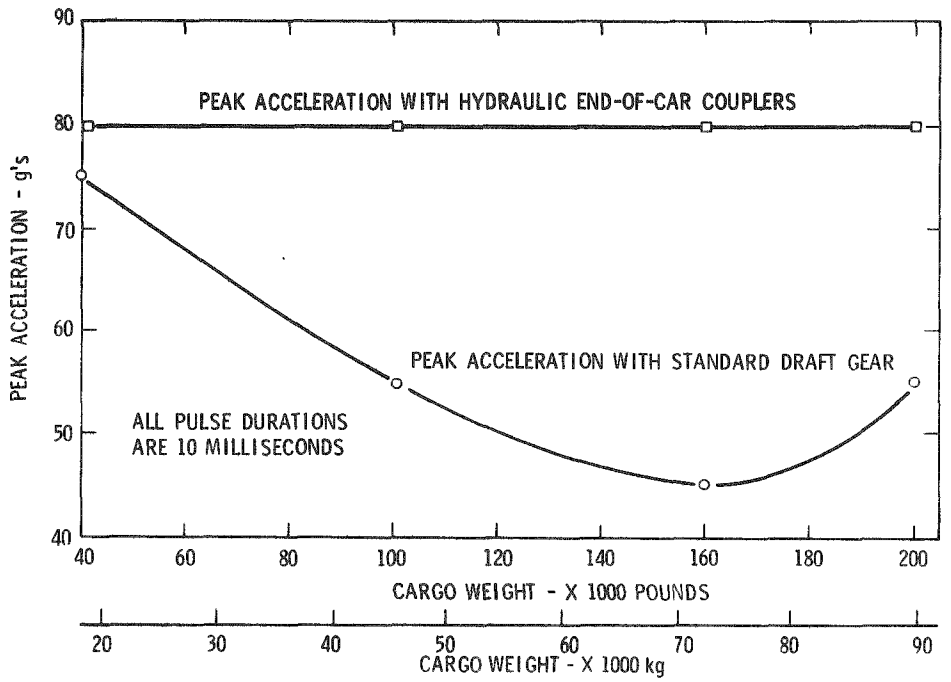

Figure 18. Peak Acceleration and Pulse Duration
Half-Sine Pulses - ATMX System
Longitudinal Axis

The curves in Figure 18 show that, if improperly matched end-of-car couplers and tiedown stiffnesses are used, the peak accelerations of half-sine pulses which envelop the response spectra are higher than those required to envelop the spectra for standard draft gear. However, when one compares the response spectra, which are shown in the Appendix (for example: Fig. A-5 & A-13), for the spent fuel system (cargo tied down) with the ATMX car using the identical end-of-car couplers and resulting spring rates, one finds that response accelerations for the spent fuel cask system are higher in most frequencies. Yet the peak accelerations of the simple input pulses are higher for the ATMX car. These higher peak accelerations are caused by the need to envelop the ATMX response spectra to 100 Hz while the spectra for the spent fuel cask system is enveloped to only 60 Hz. If the ATMX tiedown system stiffness was reduced to 75 Hz, the

peak accelerations of simple pulses to envelop the response spectra with the hydraulic end-of-car coupler would be a constant 49 g just as the tied down spent fuel cask system. If the system stiffness can be reduced further, the peak accelerations of the simple pulses would be lower.

Conclusions

Based on analytical studies conducted for this chapter the following conclusions can be drawn for 17.78 km/hr (11.05 mph) coupling velocities:

(1) Containers should be tied securely to the rail car to avoid any relative motion between the cargo and the car followed by stiff impact of the cargo against car structure.

(2) For rail cars equipped with standard draft gear, cargo response decreased as weight increased up to the point where the coupler springs bottom out. For the conventional ATMX rail car, 712,000 N (160,000 pounds) is the cargo weight which permits the most efficient use of the spring system employed in the couplers. Lighter cargo weights appear to be driven more violently because of stiffness. Heavier cargo resulted in bottoming of the coupler springs. This bottoming caused increased response in the tie-down structure.

(3) If the cargo is tied securely to the rail car and shock attenuating couplers are used, cargo weight has little effect on the cargo response to coupling impacts. Matching the end-of-car coupler to the cargo weight as well as tuning the tie-down stiffness would decrease the peak acceleration level to the cargo.

(4) Each transportation system, consisting of a rail car, container, and tie-down structure, form a dynamic system which is best studied and analyzed on an individual basis. Results from general studies of the type presented in this report cannot treat all of the design-dependent detail that will vary from one system to another. The analytical procedures employed here are applicable, however, and may be useful for more precise investigations of specific systems.

References

1. Summary of Data from Truck Shipment of a Uranium Cask from Oak Ridge, Tennessee to Paducah, Kentucky. Data Bank Entry No. 1313.

2. Transportation Dynamic Environment Summary, January 1973, Data Bank Entry Number A1354, is a summary which resulted from assembling, collating, and interpreting all the transportation vibration and shock data placed in the data bank from its inception in 1960 through January 1973.

3. Paper presented at 16th Annual Technical Meeting, Institute of Environmental Sciences; April 1970. "Report on Rail Shipment of a Cask between Paducah, Kentucky and Oak Ridge, Tennessee." Data Bank Entry Number 1320.

4. Report No. FRA-RT-70-26, DOT Contract No. DOT-FR-9-0038, dated August 1970, Robert W. Luebke, Chesapeake and Ohio Railway/ Baltimore and Ohio Railroad. Data Bank Entry 1328.

5. Extraction from Shock and Vibration Bulletin 33, Part II, 1964, L. W. Lahood, Raytheon. Data Bank Entry Number 289.

6. Extraction from Observed Switching Speeds Empty and Loaded Cars - Erie R.E. Co., Hammond Yard; Indiana Harbor Belt R.R. Co., Gibson Yard; Illinois R.R., Markham Yard. Data Bank Entry No. 286.

7. Extraction from the Railroad Environment, Technical Research Department, New York Central Railroad, 1960. Data Bank Entry Number 1118.

8. Extraction from Shock and Vibration Handbook, Volume 3, 1961, Occurrence of Rail Switching Shock. Data Bank Entry Number 287.

9. Specifications for Design, Fabrication and Construction of Freight Cars, Association of American Railroads, Chicago, Ill., Sept. 1, 1964.

10. ATMX-600 Railcar, A New Concept in Radioactive Waste Shipments, Frank E. Adcock, Proceedings Third International Symposium Packaging and Transportation of Radioactive Materials, August 16-20, 1971, 71501 (Vol. 1), Richland, Washington Conference.

APPENDIX

COMPUTER-GENERATED RESPONSE SPECTRA

Response spectra generated by analysis of the spring-mass models discussed in Chapter III are presented in this Appendix. They result from analysis of response of the models to shock caused by rail coupling. The impact velocity used in the analysis was 17.78 km/hr (11.05 mph). Cargo weight was varied from 178,000 to 890,000 N (40,000 to 200,000 pounds).

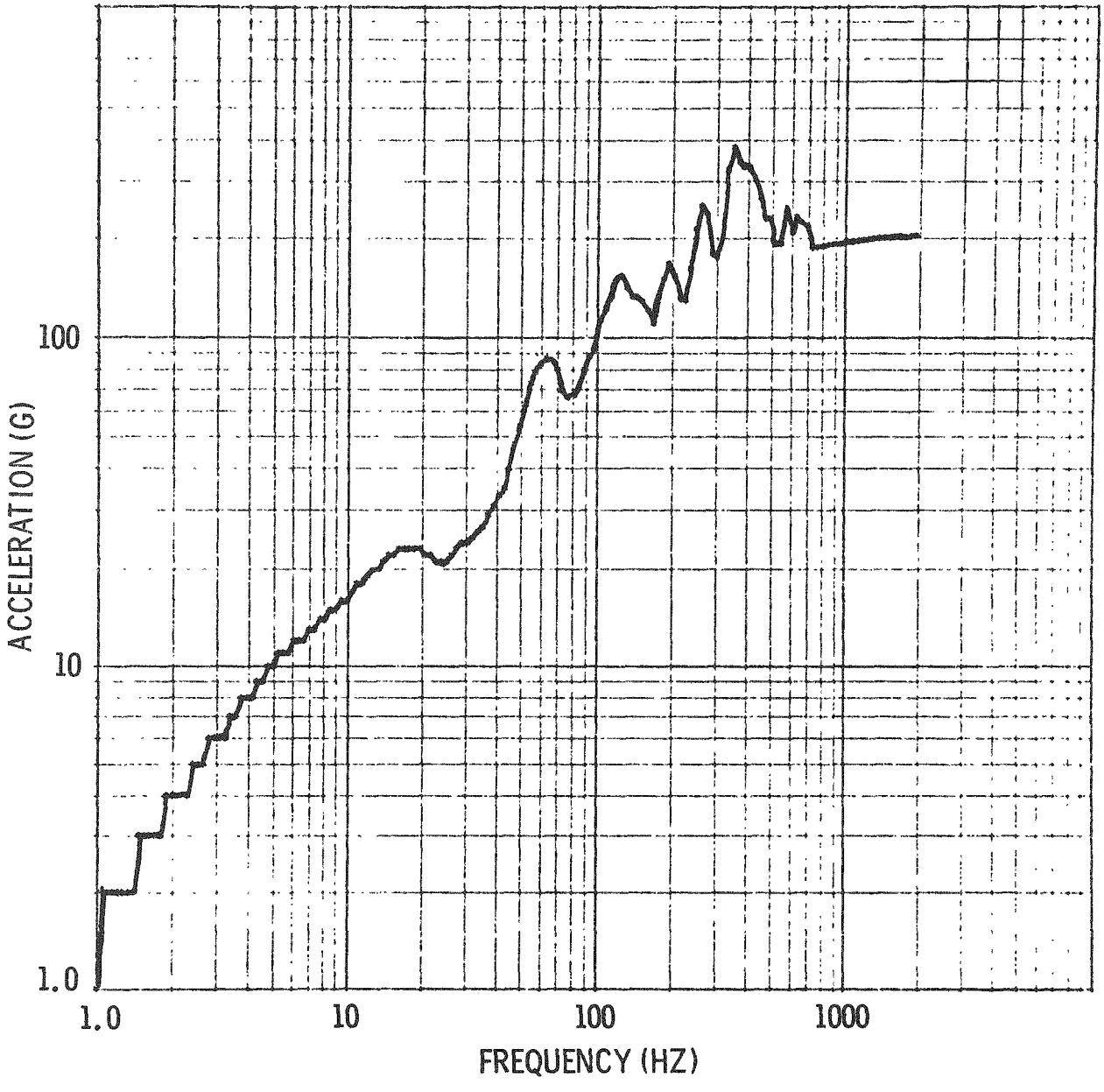

Figure A-1. Response Spectrum Analytical Results

Spent Fuel Cask System with 3.2 mm (1/8 inch) Spacing, 178,000 N (40,000 pound) Cargo, 17.78 km/hr (11.05 mph) Impact Velocity, 3 percent Damping, Longitudinal Axis

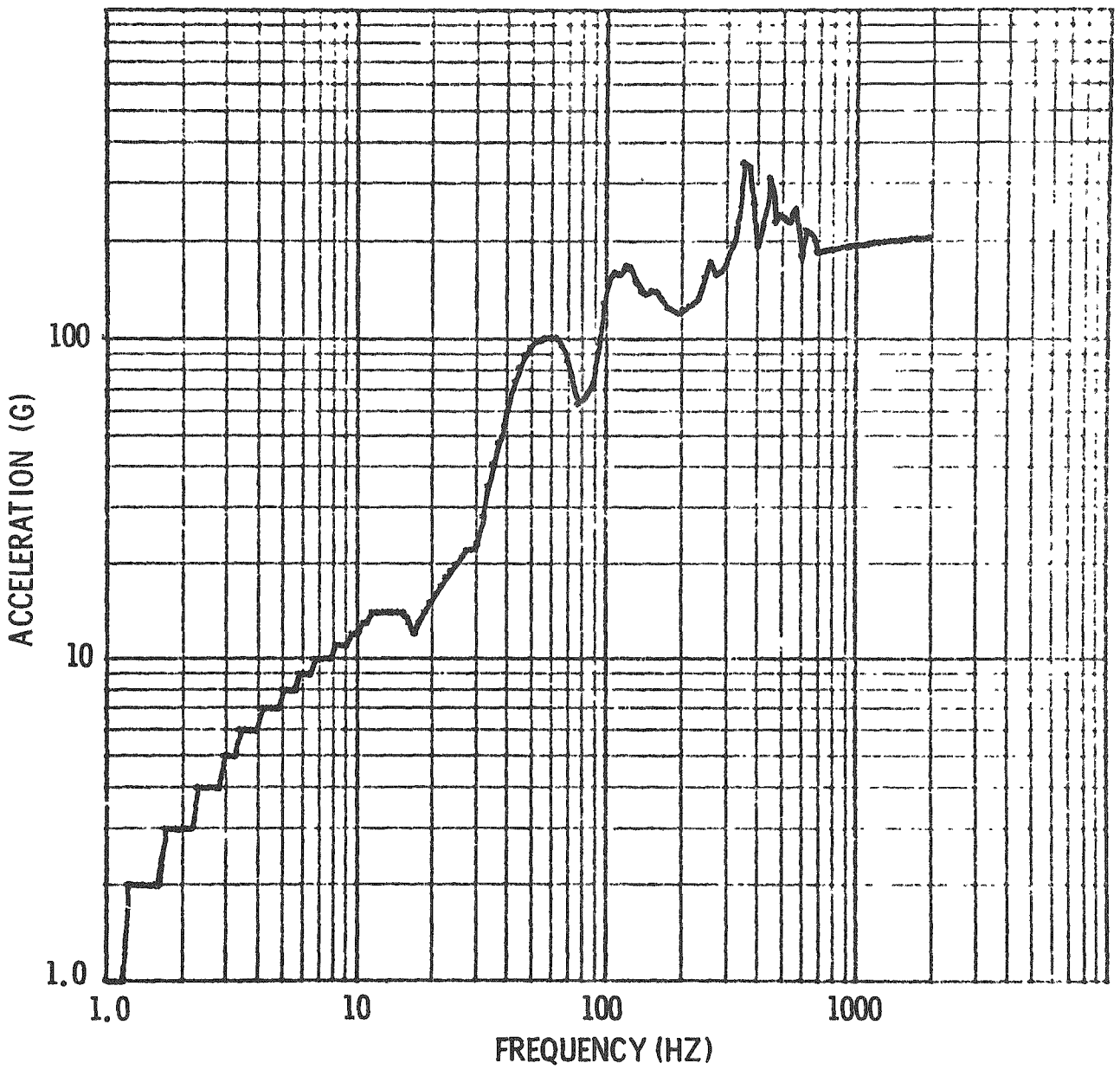

Figure A-2. Response Spectrum Analytical Results

Spent Fuel Cask System with 3.2 mm (1/8 inch) Spacing, 445,000 N (100,000 pound) Cargo, 17.78 km/hr (11.05 mph) Impact Velocity, 3 percent Damping, Longitudinal Axis

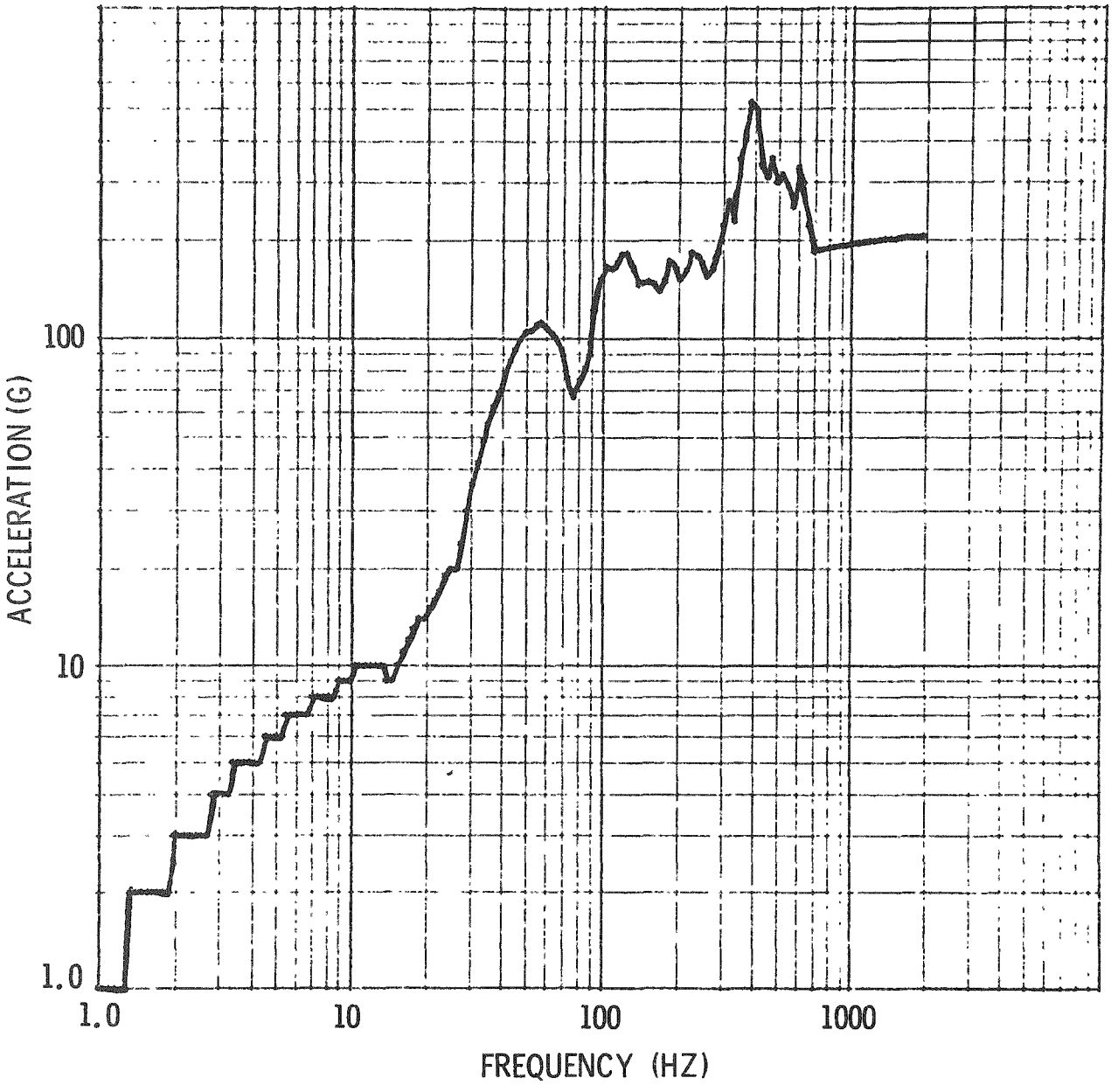

Figure A-3. Response Spectrum
Analytical Results

Spent Fuel Cask System with 3.2 mm (1/8 inch) Spacing, 712,000 N (160,000 pound) Cargo, 17.78 km/hr (11.05 mph) Impact Velocity, 3 percent Damping, Longitudinal Axis

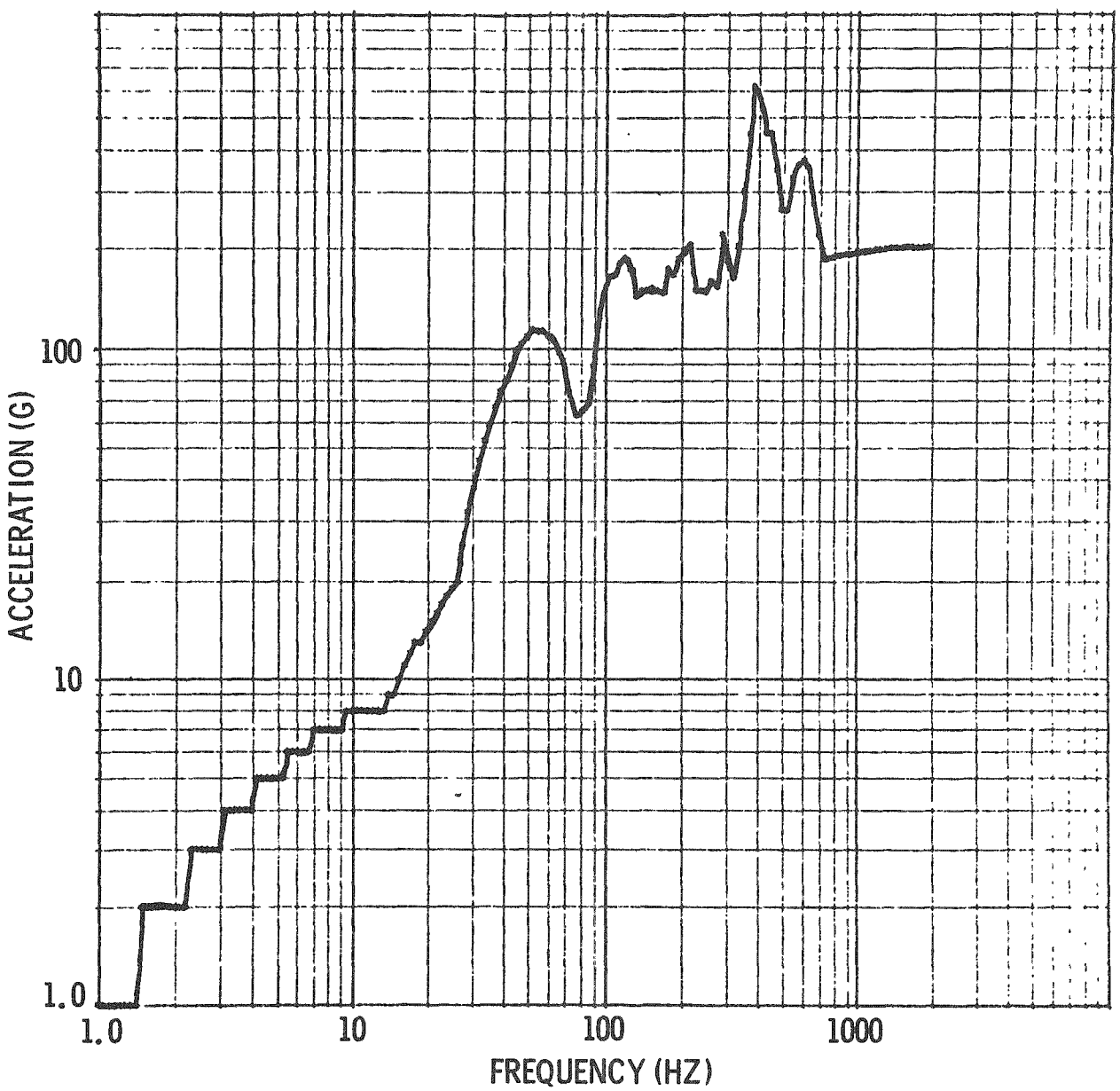

Figure A-4. Response Spectrum Analytical Results

Spent Fuel Cask System with 3.2 mm (1/8 inch) Spacing, 890,000 N (200,000 pound) Cargo, 17.78 km/hr (11.05 mph) Impact Velocity, 3 percent Damping, Longitudinal Axis

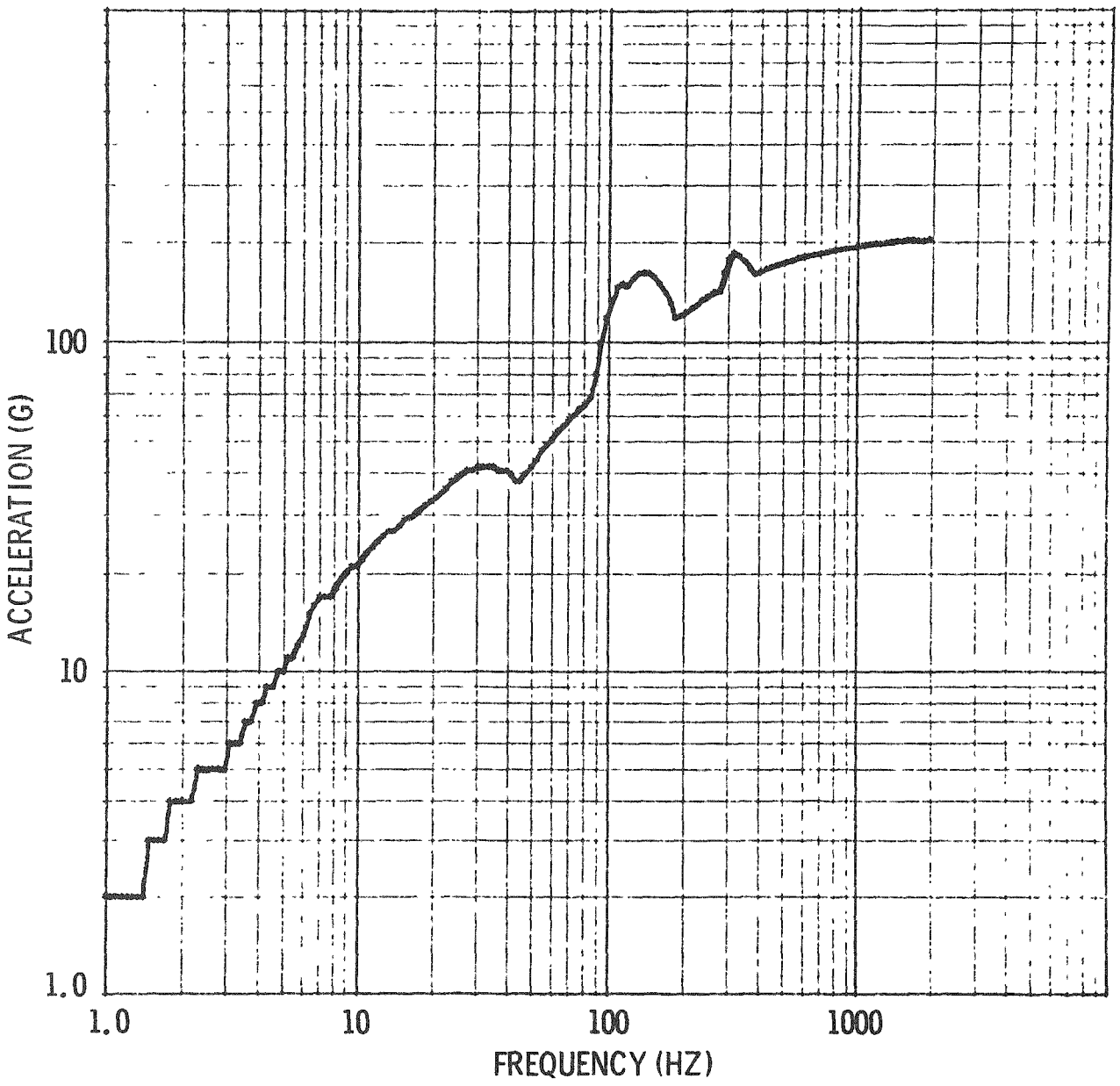

Figure A-5. Response Spectrum
Analytical Results

Spent Fuel Cask System, Cargo Tied Down, 178,000 N (40,000 pound) Cargo, 17.78 km/hr (11.05 mph) Impact Velocity, 3 percent Damping, Longitudinal Axis

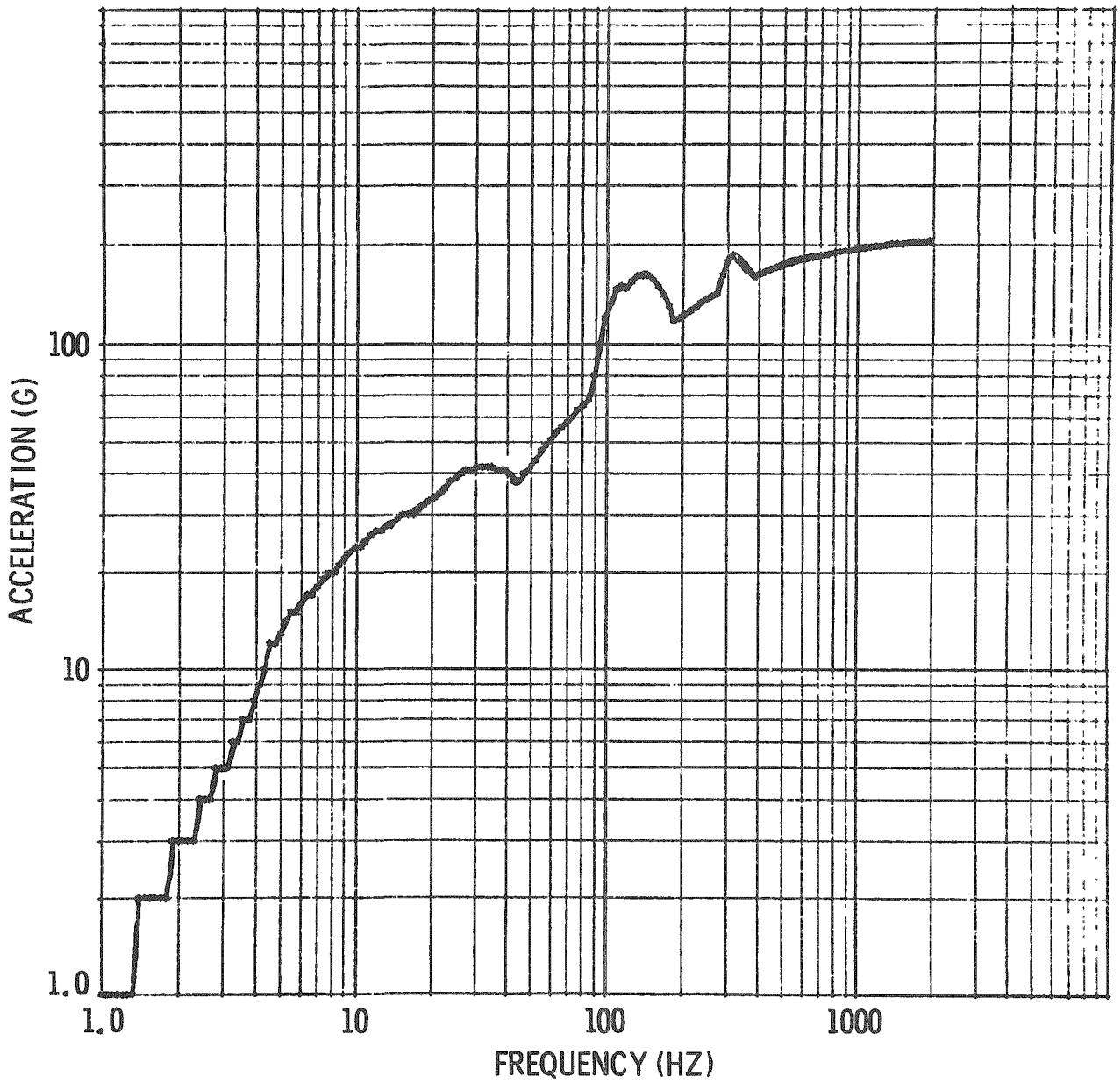

Figure A-6. Response Spectrum
Analytical Results

Spent Fuel Cask System, Cargo Tied Down, 445,000 N (100,000 pound) Cargo, 17.78 km/hr (11.05 mph) Impact Belocity, 3 percent Damping, Longitudinal Axis

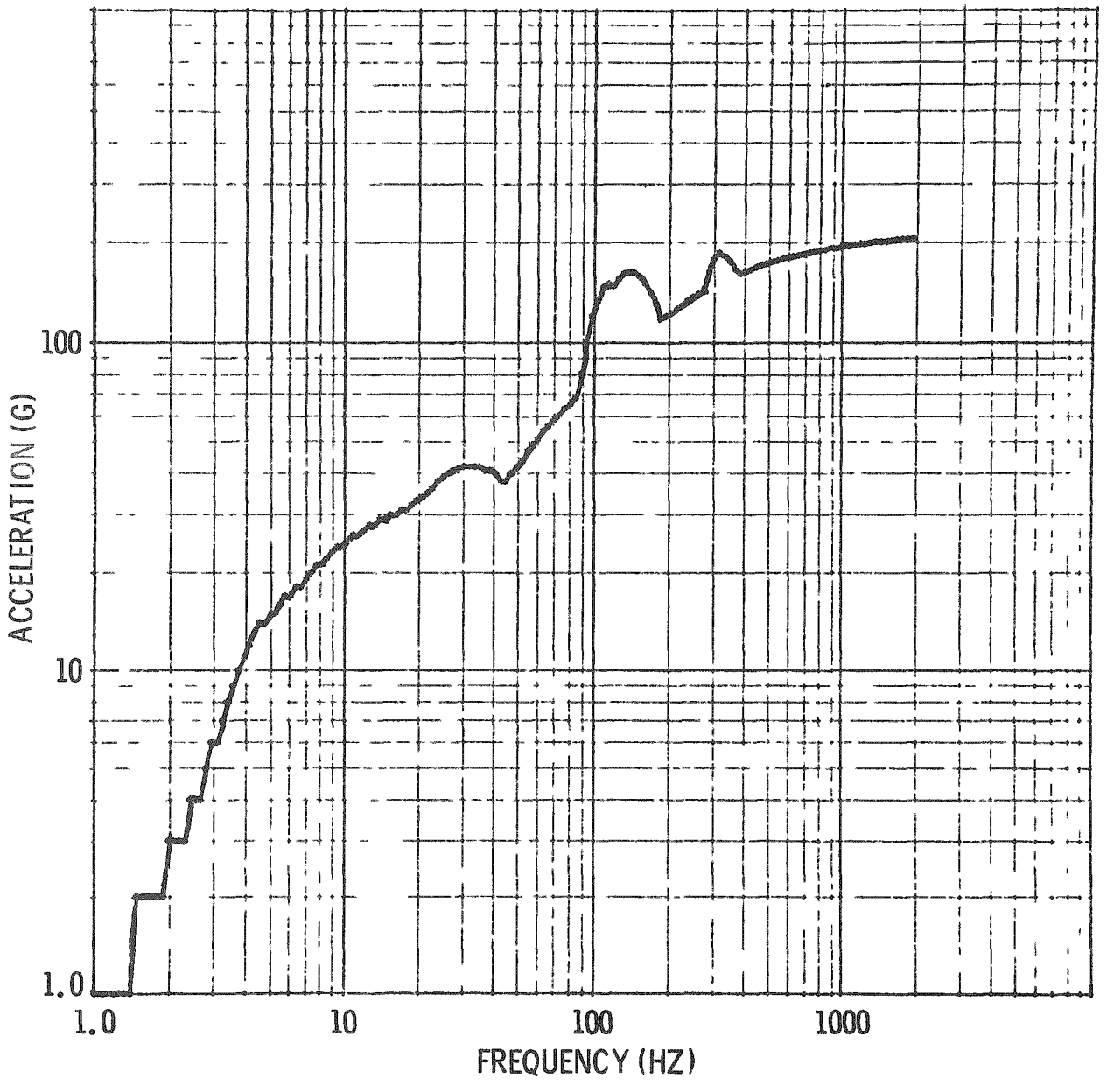

Figure A-7. Response Spectrum Analytical Results

Spent Fuel Cask System, Cargo Tied Down, 712,000 N (160,000 pound) Cargo, 17.78 km/hr (11.05 mph) Impact Velocity, 3 percent Damping, Longitudinal Axis

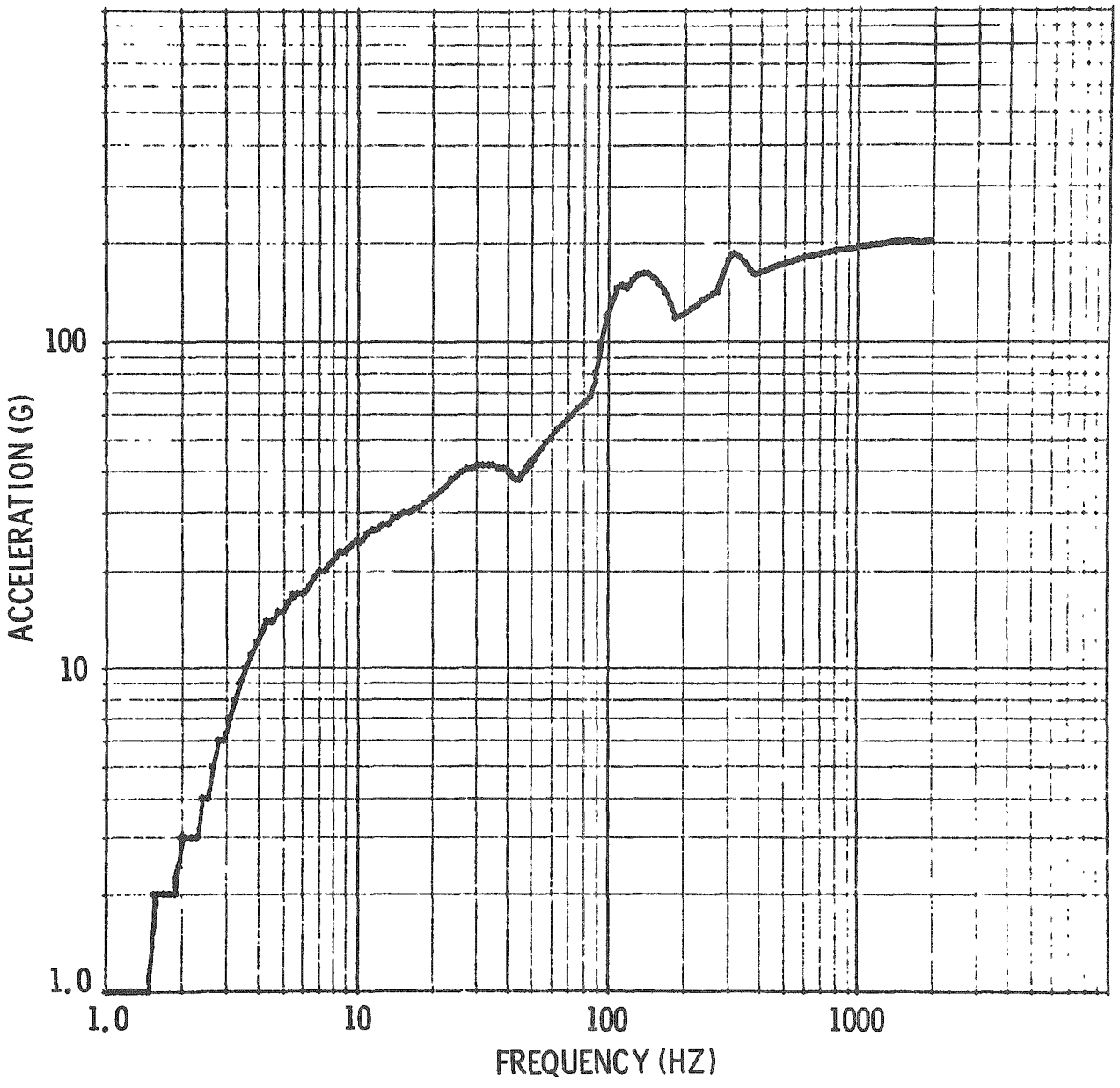

Figure A-8. Response Spectrum
Analytical Results

Spent Fuel Cask System, Cargo Tied Down,
890,000 N (200,000 pound) Cargo, 17.78 km/hr
(11.05 mph) Impact Velocity, 3 percent
Damping, Longitudinal Axis

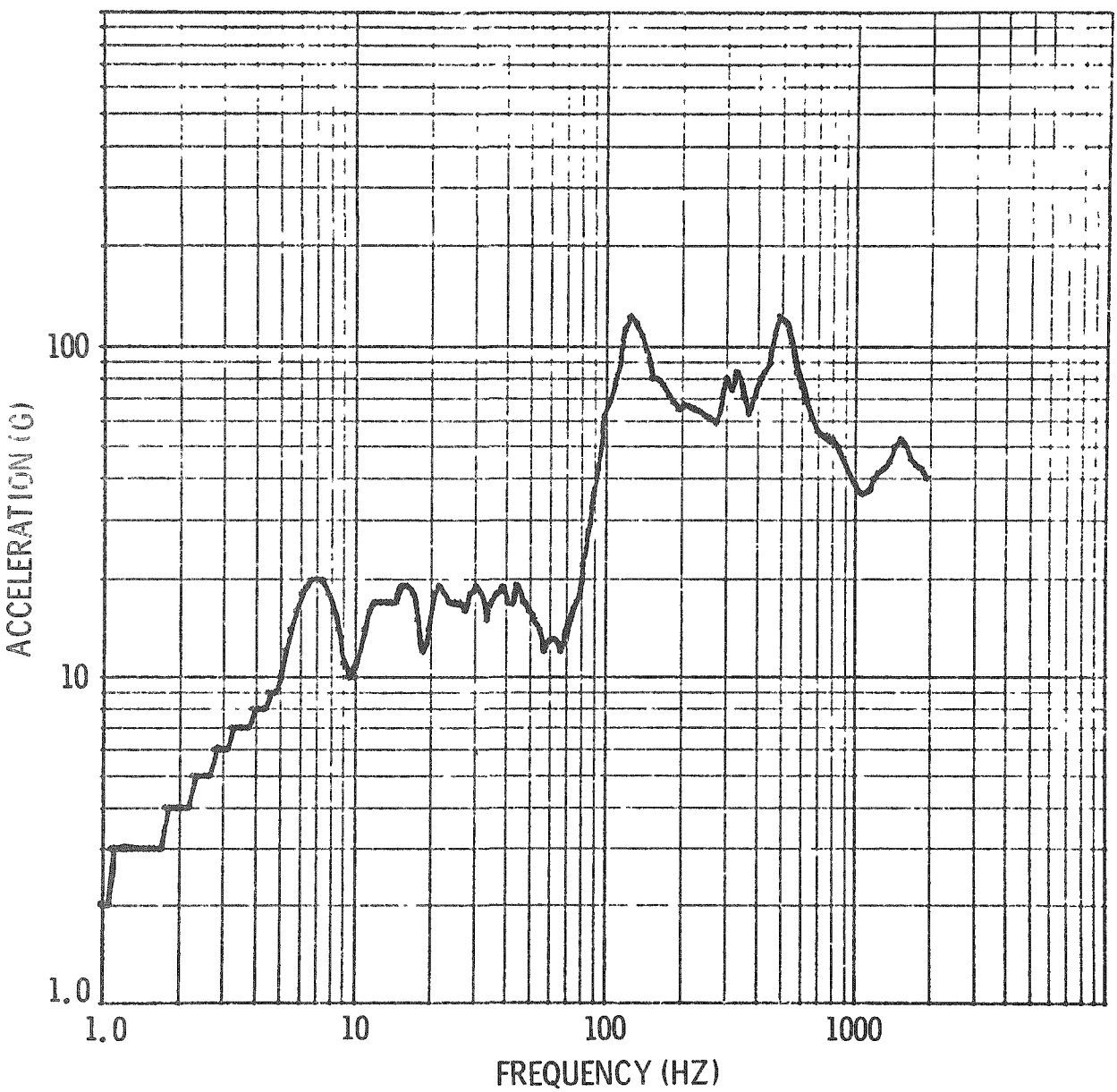

Figure A-9. Response Spectrum Analytical Results

ATMX Car, Standard Draft Gear, 178,000 N (40,000 pound) Cargo, 17.78 km/hr (11.05 mph) Impact Velocity, 3 percent Damping, Longitudinal Axis

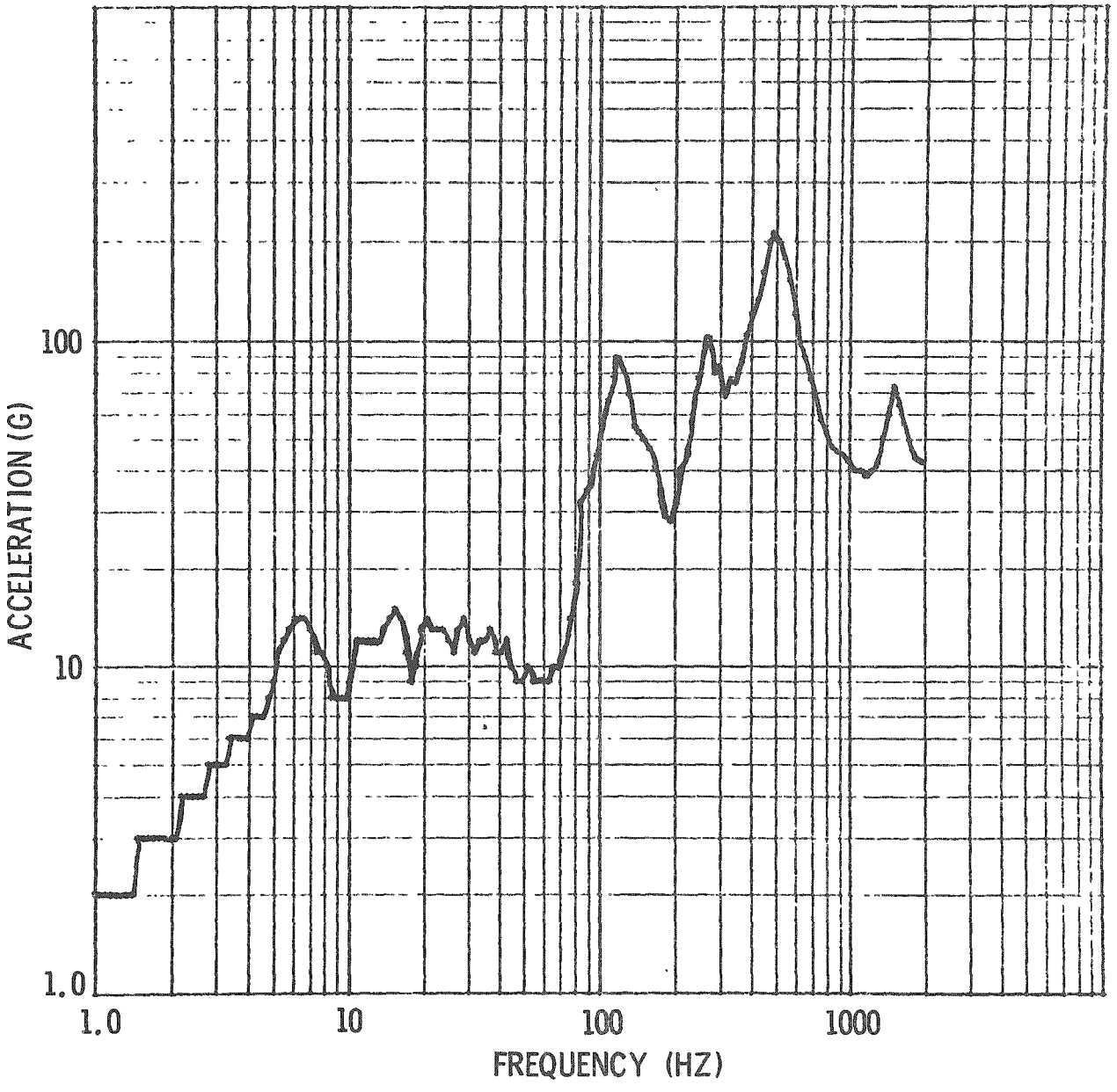

Figure A-10. Response Spectrum Analytical Results

ATMX Car, Standard Draft Gear, 451,000 N (101,300 pound) Cargo, 17.78 km/hr (11.05 mph) Impact Velocity, 3 percent Damping, Longitudinal Axis

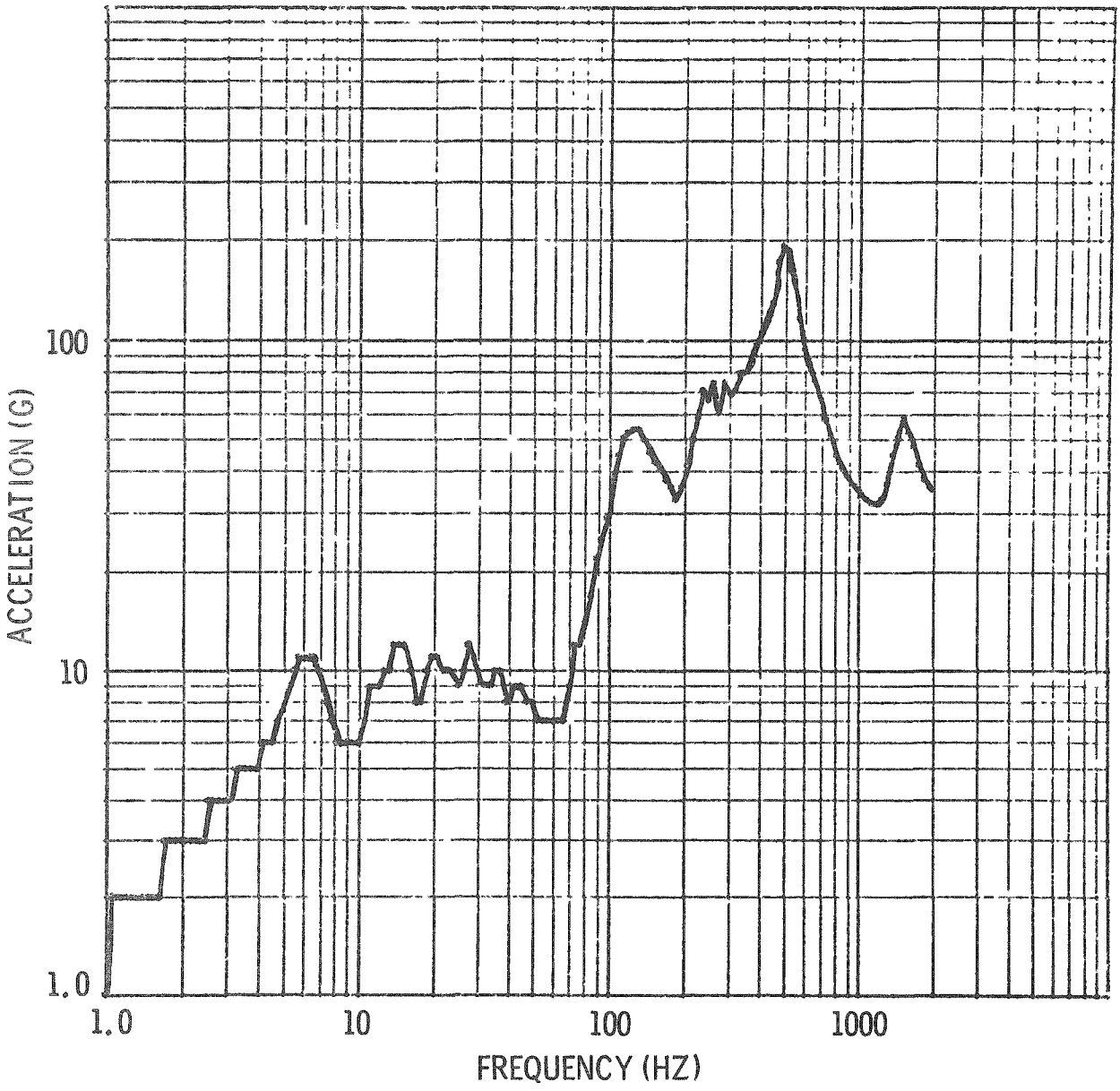

Figure A-11. Response Spectrum Analytical Results

ATMX Car, Standard Draft Gear, 712,000 N (160,000 pound) Cargo, 17.78 km/hr (11.05 mph) Impact Velocity, 3 percent Damping, Longitudinal Axis

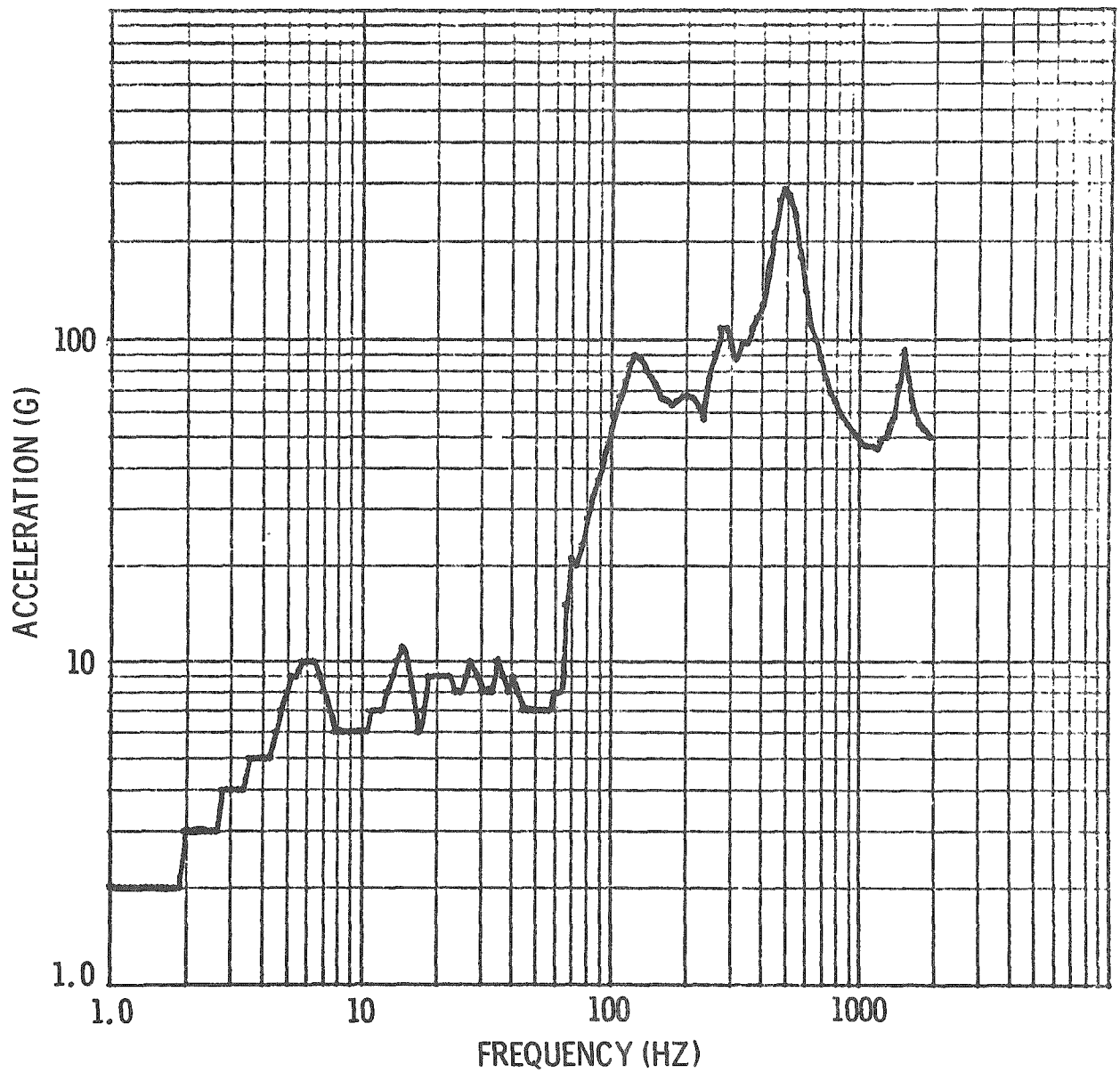

Figure A-12. Response Spectrum Analytical Results

ATMX Car, Standard Draft Gear, 890,000 N (200,000 pound) Cargo, 17.78 km/hr (11.05 mph) Impact Velocity, 3 percent Damping, Longitudinal Axis

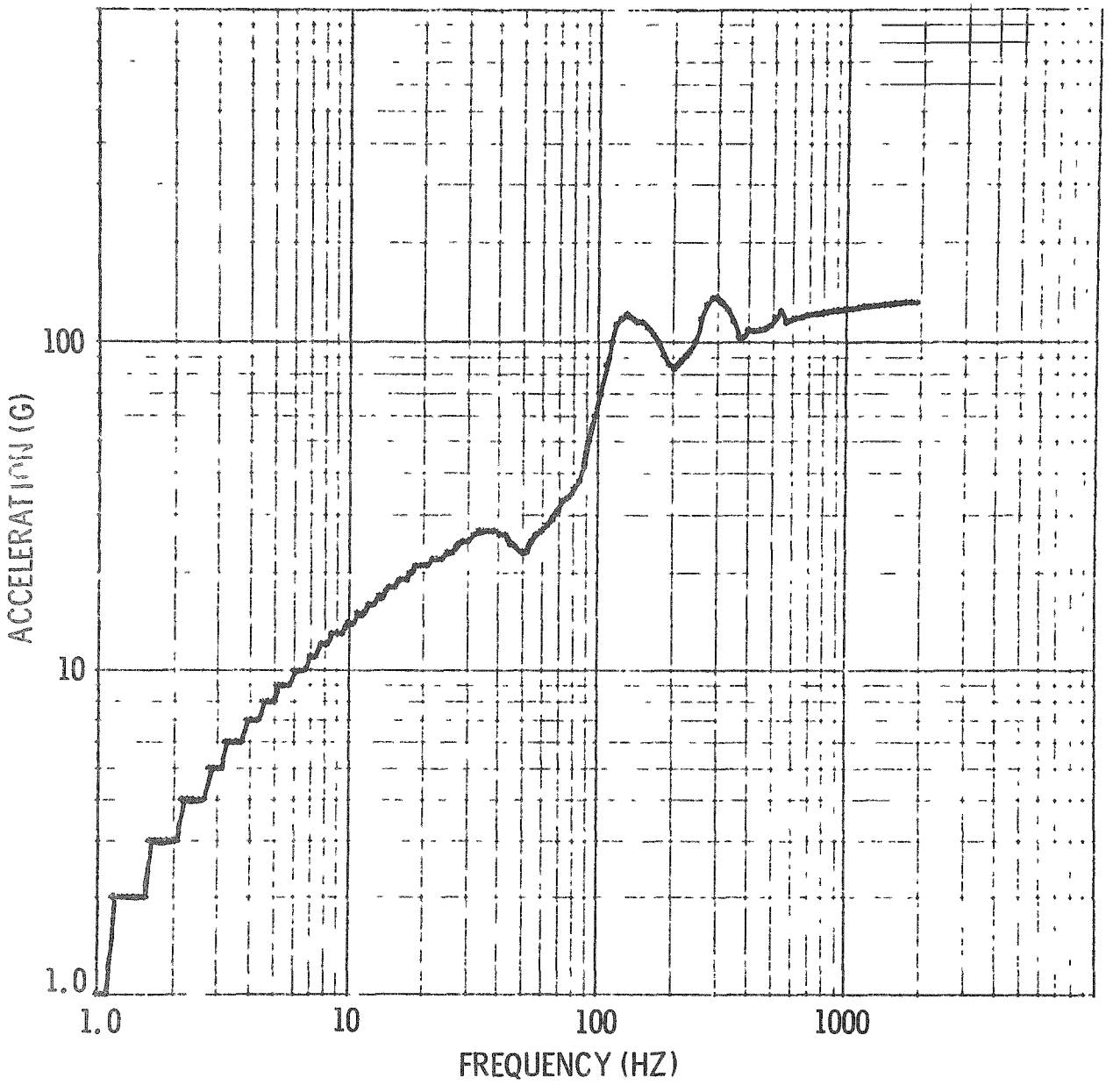

Figure A-13. Response Spectrum
Analytical Results

ATMX Car, Shock Attenuating Couplers,
178,000 N (40,000 pound) Cargo, 17.78 km/hr
(11.05 mph) Impact Velocity, 3 percent
Damping, Longitudinal Axis

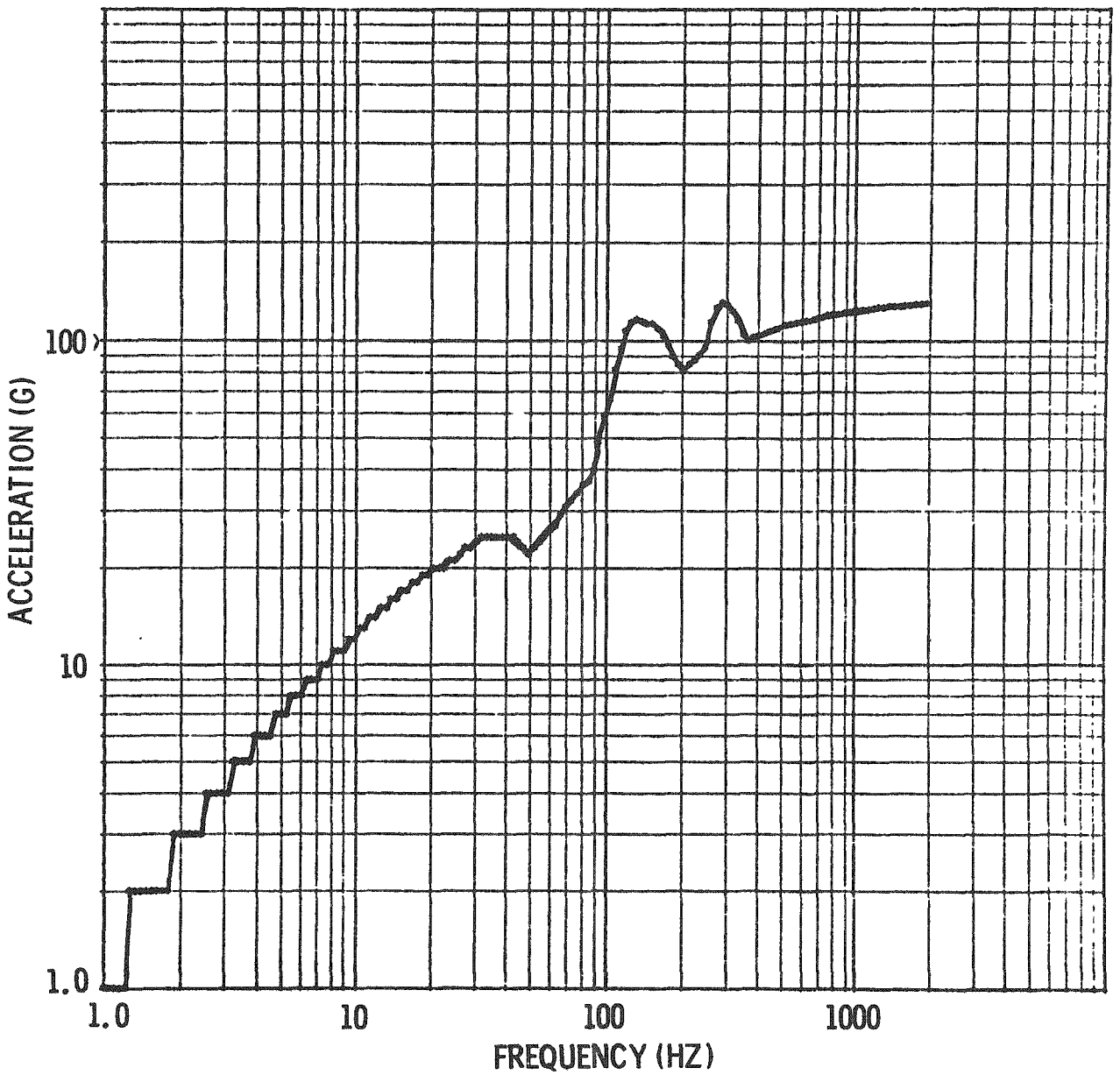

Figure A-14. Response Spectrum
Analytical Results

ATMX Car, Shock Attenuating Couplers,
451,000 N (101,300 pound) Cargo, 17.78 km/hr
(11.05 mph) Impact Velocity, 3 percent
Damping, Longitudinal Axis

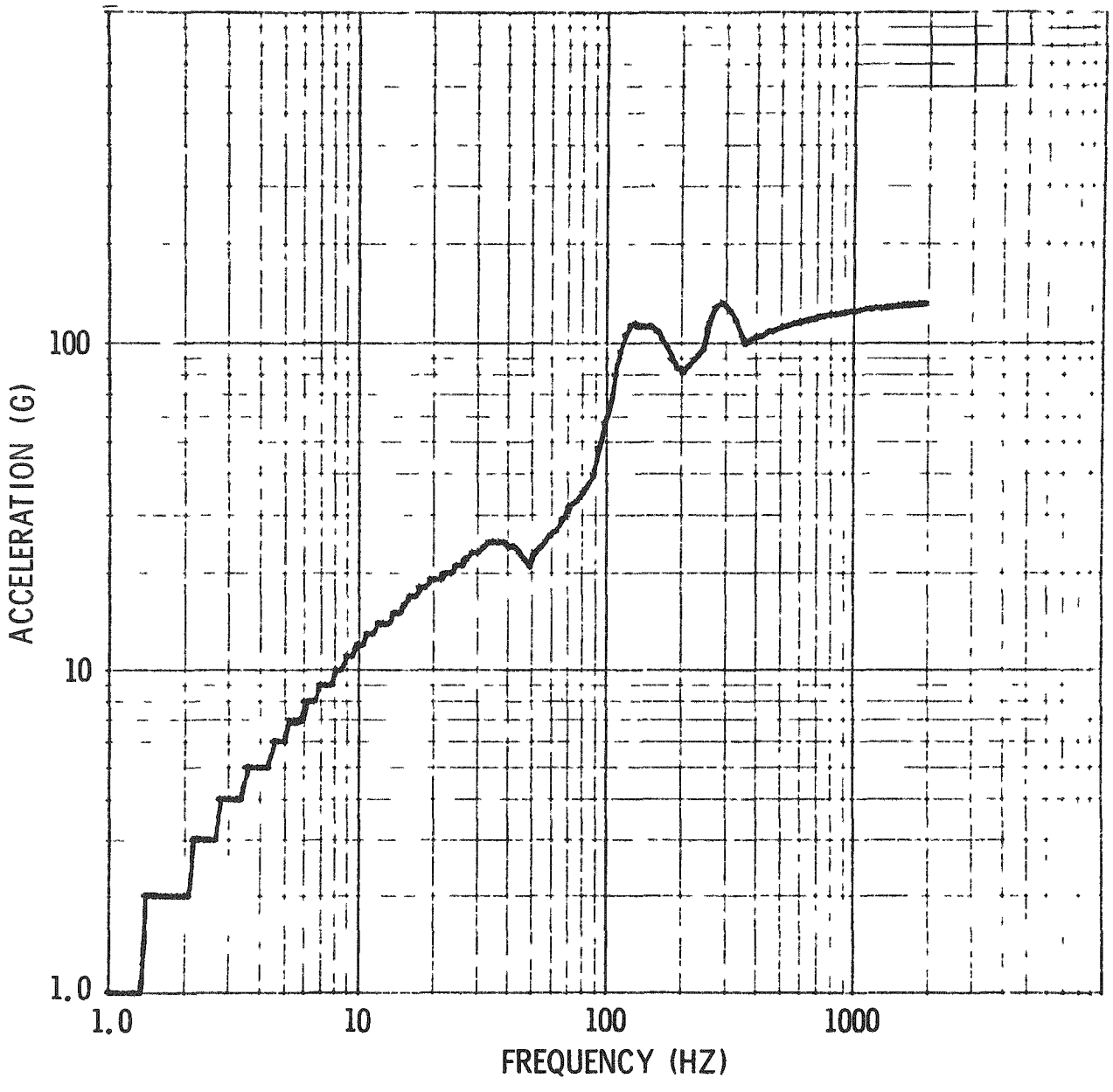

Figure A-15. Response Spectrum Analytical Results

ATMX Car, Shock Attenuating Couplers, 712,000 N (160,000 pound) Cargo, 17.78 km/hr (11.05 mph) Impact Velocity, 3 percent Damping, Longitudinal Axis

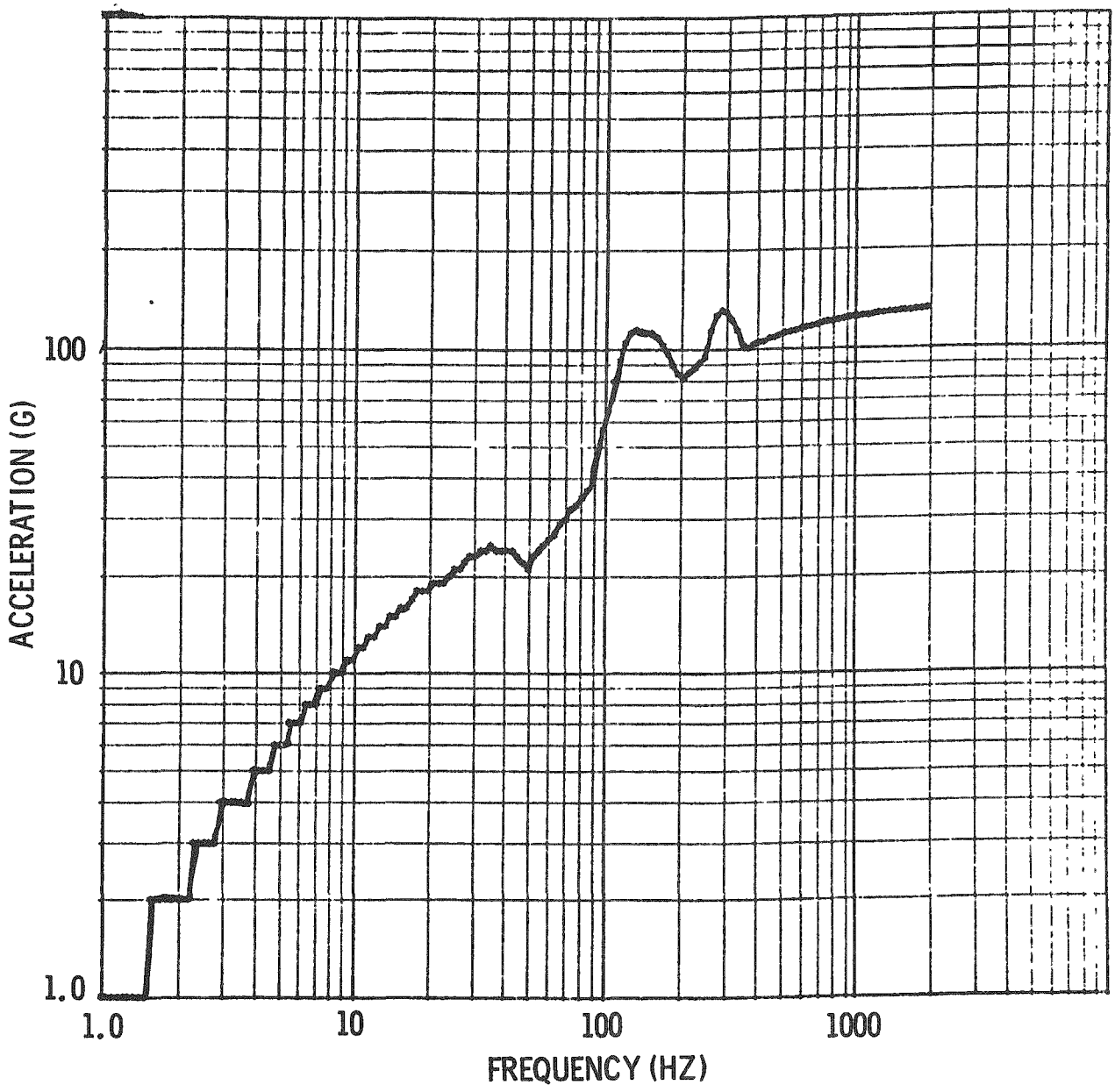

Figure A-16. Response Spectrum Analytical Results

ATMX Car, Shock Attenuating Couplers, 890,000 N (200,000 pound) Cargo, 17.78 km/hr (11.05 mph) Impact Velocity, 3 percent Damping, Longitudinal Axis

DISTRIBUTION

U. S. NRC Distribution System
Distribution Category NRC-12 (238 copies)
Attn: Robert Wade
Washington, D.C. 20555

D. A. Nowlin, Director
Special Programs Division
U. S. Energy Research and Development
Administration
Albuquerque Operations Office
Albuquerque, New Mexico 87115

William Lahs
Safer Division
U.S. Nuclear Regulatory Commission
Washington, D.C. 20555

1000	G. A. Fowler
1200	W. A. Gardner
1280	T. B. Lane
1281	S. W. Key
1282	T. G. Priddy
1282	C. F. Magnuson (10)
1284	R. T. Othmer
1284	L. T. Wilson (10)
5000	A. Narath
5100	J. K. Galt
5200	E. H. Beckner
5400	A. W. Snyder
5430	R. M. Jefferson
5431	R. E. Nickell
5431	W. A. Von Riesemann
5432	L. L. Bonzon
5432	R. E. Luna
5433	R. B. Pope
5433	J. M. Freedman
5433	H. R. Yoshimura
5700	J. M. Scott
5711	E. L. Harley
5800	R. S. Claassen
8266	E. A. Aas (2)
3141	C. A. Pepmueller/Actg/ (5)
3151	W. L. Garner (3)
	For ERDA/TIC (Unlimited Release)